

Copyright
by
Perrine Mathieu
2013

The Report Committee for Perrine Mathieu
Certifies that this is the approved version of the following report:

Mission Planning Tool for Small Satellites

APPROVED BY
SUPERVISING COMMITTEE:

Supervisor:

Glenn Lightsey

Wallace Fowler

Mission Planning Tool for Small Satellites

by

Perrine Mathieu, B.S.

Report

Presented to the Faculty of the Graduate School of

The University of Texas at Austin

in Partial Fulfillment

of the Requirements

for the Degree of

Master of Science in Engineering

The University of Texas at Austin

December 2013

Mission Planning Tool for Small Satellites

by

Perrine Mathieu, MSE

The University of Texas at Austin, 2013

SUPERVISOR : Glenn Lightsey

The Texas Spacecraft Laboratory (TSL) at the University of Texas at Austin is currently planning to launch two CubeSat missions in 2014. Innovations are more readily attempted on such low-risk small satellites than with higher-cost payloads, which puts CubeSats at the forefront of space research. The TSL CubeSats will thus be used to pioneer and demonstrate new on-orbit technology. Due to the innovative aspect of the CubeSat missions, limited prior experience exists with the technology used. It is thus important to have an accurate understanding of mission operations prior to launch through computer simulation. In order to improve the success and reliability of current and future TSL missions, a MATLAB tool was developed to simulate on-orbit operations. The various capabilities of the user-friendly tool developed include power budget calculations, pass determination and orbit simulation. The comprehensive program can predict the life of the spacecraft at critical moments of its operation and, in general, help improve understanding of how to successfully meet mission requirements and design mission operations.

Table of Contents

1	Introduction	1
2	Description of Tool and Models	2
2.1	Program Description and Architecture	2
2.2	User Interface	6
2.3	Program Outputs	10
2.4	Orbit Propagation and Perturbations	15
2.5	Satellite Geometry and Power generation	16
3	RACE Mission	20
3.1	RACE Mission Requirements and Radiometer Instrument	20
3.2	RACE Power System	21
4	Validation	22
4.1	Overhead Passes	22
4.2	Power Generation and Attitude Validation	26
5	Results and Discussion	35
5.1	Sunlight	35
5.2	Radiometer Experiment	38
6	Conclusion	56
	References	57

1 Introduction

The UT-Austin Texas Spacecraft Laboratory (TSL), designs, builds and researches the technology of small satellites, known as CubeSats. CubeSats are low-risk small satellites of standardized dimensions that are becoming increasingly popular for space research. Their small sizes of typically a few standard units, with 1U being a volume of 10x10x11 cm, reduces launch costs, letting them ride at low cost as secondary payloads. Additionally, their simplified design reduces the development time making them ideal candidates for innovation and space research that is not as readily attempted with large higher-cost payloads.

The TSL is currently building two 3U cubesats due to launch in 2014, Bevo-2 and RACE. Bevo-2, part of the collaborative NASA Johnson Space Center LONESTAR project (Low-Earth Orbiting Navigation Experiment for Spacecraft Testing Autonomous Rendezvous and Docking) will demonstrate various Cubesat innovative technologies and demonstrate proximity operations. The Radiometer Atmospheric CubeSat Experiment (RACE) mission, a collaboration with the Jet Propulsion Laboratory (JPL) will perform the spaceborne validation of new radiometer instrument technology. Both missions will aid in reducing the risk of future users of the innovative technologies they pioneered.

In order to improve the success and reliability of the missions designed, an accurate understanding of the on-orbit operations of the spacecraft is essential. A tool was developed to that purpose, to simulate the on-orbit operations and capabilities of the spacecraft and gain a better understanding of how to meet mission requirements. This tool is useful for both current and future spacecraft and can, for example, simulate a day in the life of a spacecraft at a critical moment of its operation. The various capabilities span aspects of different satellite systems including power budget calculations, ground station pass determination and orbit simulation. This versatile and modular tool can be easily adapted to fit different missions to better design and predict on-orbit operations, which is critical to successful mission design. Future students may thus continue to modify and develop the tool, increasing its capabilities over time.

2 Description of Tool and Models

This section acts as a user guide and explains how the program is organised, the different models used and the assumptions made in the calculations. The program was written in MATLAB and was coupled with the JPL Spice Toolkit, a NASA information system providing access to “Ancillary data”, such as planetary ephemerides or atmospheric models [1]. The entire program is intended to be user friendly and is located in a folder that can be easily moved/transferred without affecting its integrity for the benefit of new users.

2.1 Program Description and Architecture

The general program architecture is represented in Figure 1, showing the relationship with outside program components. In addition to the Matlab functions that were specifically written for this program, the program interacts with the JPL Spice Toolbox which was downloaded and included in the program folder. The program can thus make use of data and functions made accessible to the public by JPL, for example planetary ephemeris. Furthermore, two different methods are available for the user to interact with the tool. The first involves a GUI and the other a Matlab m-file which is directly modified. Further details are given on the user interface in section 2.2. The user can further modify satellite parameters such as power data directly in an Excel Sheet designed by the TSL. Thus, the program reads power data from the Excel spreadsheet specific to each mission. The user can consequently run the program smoothly using one of the two input methods and modify additional power parameters directly in Excel without having to modify the code.

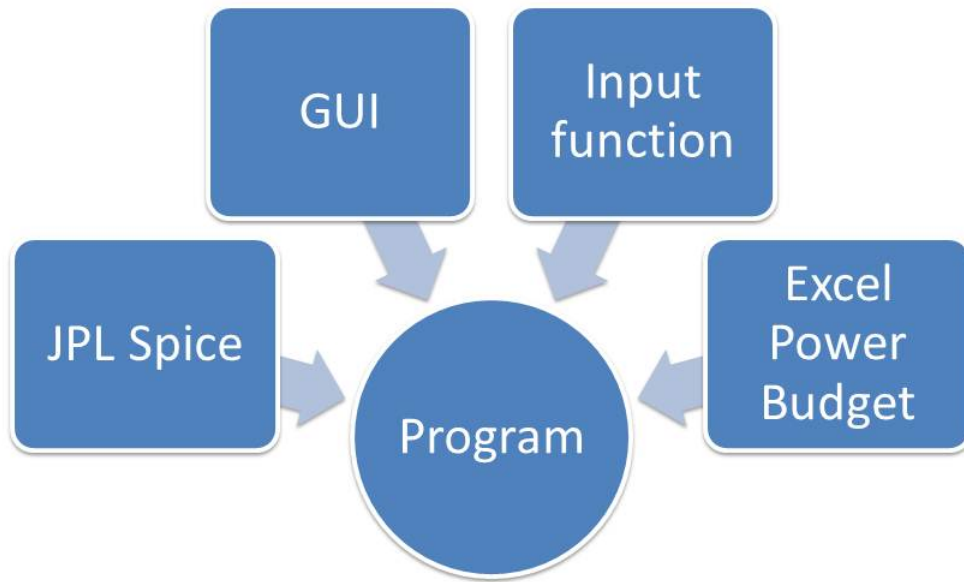


Figure 1: *Program General Architecture*

Figure 2 details the architecture of the main Matlab functions written with the arrows showing the direction of function dependencies. Essentially, functions located on the left call functions on their right. Note that additional functions exist which are shown in the “Additional Supporting Functions” section. These functions are utilitarian and called throughout the program for orbit parameter conversions or frame conversions. A description of these functions is given in Table 1. Both input functions are shown in light blue and call the same *Main* function which acts as the program skeleton. The input functions are thus interchangeable and can be chosen at the user’s discretion.

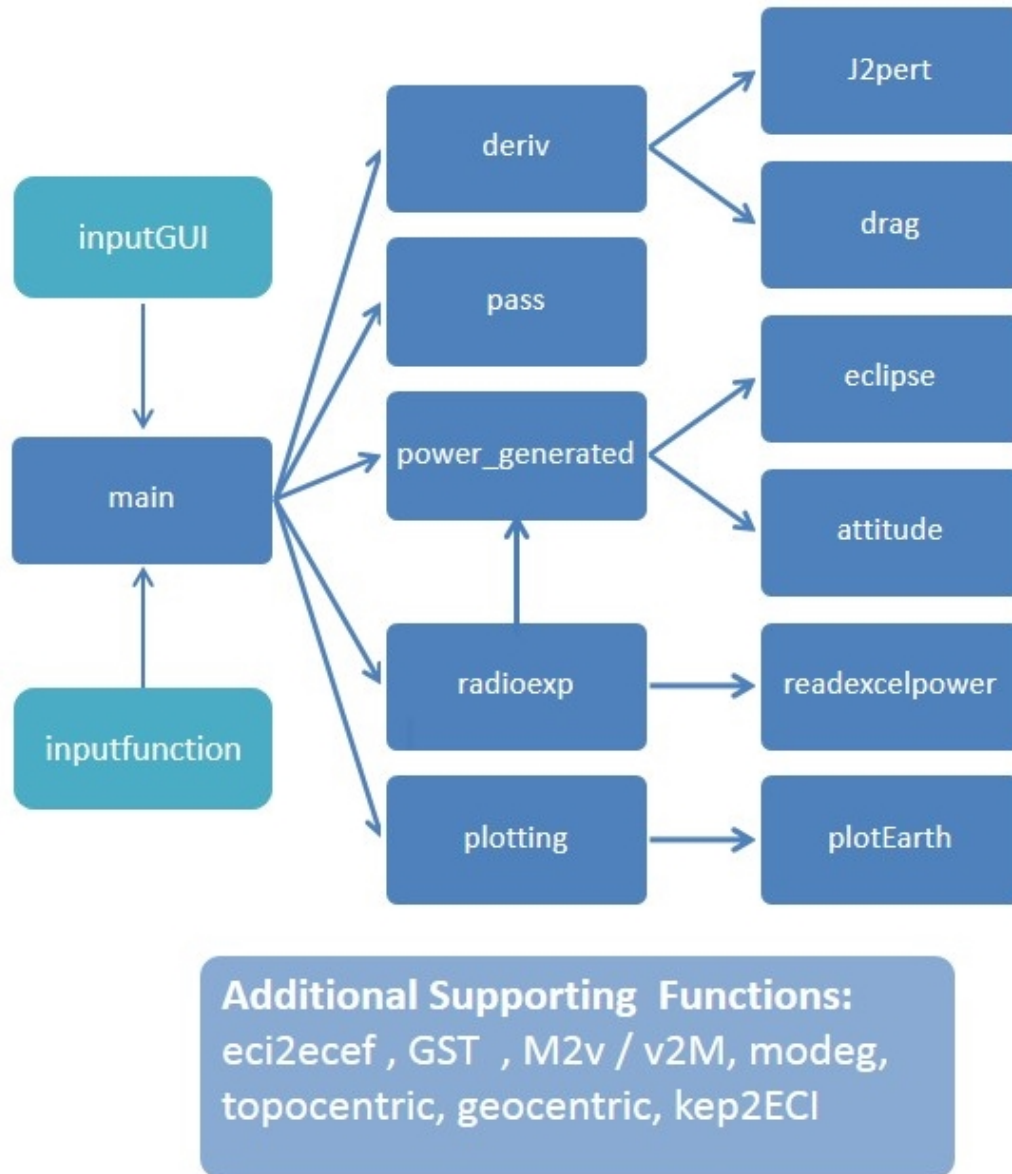


Figure 2: *Program Function architecture and dependence*

The top to bottom diagram organisation of Figure 2 gives an idea of the chronology of the program. Once the user input is defined and the *Main* is executed, the program begins with the *deriv* function which propagates the two-body orbit numerically accounting for perturbations if needed. The program then determines ground passes of the spacecraft and

Function Name	Description
eci2ecef	Converts a Position vector in ECI frame (Earth Centered Inertial) to a position vector in ECEF (Earth Centered Earth Fixed) frame. [2]
GST	Converts a Julian date at 0h of the day to Greenwich Sidereal time, ie. computes the westward angle from Greenwich Meridian (ECEF X-axis)to ECI X-axis [2]
M2v	Takes as input the Mean anomaly and eccentricity and outputs the True anomaly [3]
v2M	Takes as input the True anomaly and eccentricity and outputs the Mean anomaly
modeg	For an angle in degrees, returns the equivalent angle in the range -180° to 180°
topocentric	Converts a satellite position from ECEF frame to topocentric frame centered at specified station location
geocentric	Returns geocentric coordinates latitude, longitude and height from ECEF coordinates
kep2ECI	Converts Keplerian orbital elements (semi-major axis, eccentricity, inclination, argument of perigee, right ascension of ascending node and mean anomaly) to cartesian position vector in ECI frame

Table 1: Description of Supporting Functions

calculates the power generated using the positions determined in the previous orbit calculation. In order to calculate the power generated, the program accounts for the satellite geometry and user-defined attitude. Next, the program optionally calls the *radioexp* function and simulates the spacecraft life in a determined operational phase of the mission. The *radioexp* function is specific to the RACE spacecraft but a similar function can be adapted to a different mission phase or spacecraft. The modularity of the program enables future users to create their own mission plan and add it to the program. Finally the plotting is performed which gives the user visual information on the mission (eg. power generated over time, duration of ground passes, eclipse periods).

2.2 User Interface

As previously mentioned, two input methods are available for the user to interact with the program in a straightforward manner. A Matlab function called *inputfunction* can be used or, alternatively, a GUI called *inputGUI*. Both methods can be used interchangeably since they both call the same main function. In order to get started with the program, the user must open the program file path in the current Matlab workspace. This directory includes all functions written for the code with additional folders linking to modules and toolboxes developed externally. This same directory contains the power data sheet necessary for on-orbit power budget simulations, entitled `sys-budg-RACE_power.xlsx`. Figure 3 is a snapshot showing part of the power budget sheet created by the TSL for the RACE spacecraft in a particular mode of the science experiment phase of the mission.

			Transition to Radiometer Experiment Mission Script			
Subsystem Power (A)			3.3	5	Raw Bus	Total W
ADC						
	Actuators					
		Reaction Wheels	0	0.147	0	0.735
		Magnetic Torque Rods	0	0.126	0	0.63
	Sensors					
		Sun Sensors	0	0.0546	0	0.273
		Magnetometer	0	0.0525	0	0.2625
		Gyroscopes	0	0.1386	0	0.693
	Flight Computer					
		Flight Computer	0.3045	0	0	1.00485
		Kraken Interface Board	0	0	0	0
CDH	CDH Computer	Complete CDH	0.243075	0	0	0.8021475
COM						
	UHF/VHF Radio					
		Radio	0.105	0	0.2819	4.5465
	ISIS Antenna Deployment System					
		ISIS Antenna	0	0	0	0
EPS	Main EPS	EPS	0	0	0.008808725	0.13125
Radiometer	RM	RM	0	0	0	0
Allocated Current			0.652575	0.5187	0.2907	9.0782475
Maximum Current			2.5	2.5	4	80.35
Margin			1.847425	1.9813	3.7093	71.2717525
Margin (%)			73.90%	79.25%	92.73%	88.70%
	Total W for each mode					

Figure 3: Power budget example of RACE spacecraft in experiment mode

Modifications to the power values can be made to this sheet as the spacecraft undergoes further testing without affecting the program operation. The program reads only the power values for each mode highlighted in purple. Note that this sheet is not necessary if the user only wants to simulate the orbit to get information on passes, power generated, location, without studying a particular mode of operation.

Next, if the user decides to use the GUI the following command must be entered in the Matlab Command Window: `>> inputGUI` This will prompt the program to open the GUI shown in Figure 4.

The figure shows a MATLAB GUI titled "inputGUI" with the following sections and controls:

- Orbit Parameters:**
 - Semi-major axis: 6.7981363e+06 meters
 - Eccentricity: 0
 - Inclination: 52 degrees
 - Argument of Perigee: 0 degrees
 - Right Ascension of Ascending Node: 0 degrees
 - Mean Anomaly: 0 degrees
 - True Anomaly: 0 degrees
- Ground Station Parameters:**
 - location coordinates: ☒ UT Austin, ☐ Other (30.287° N, -97.735° E, 15 meters altitude)
 - minimum elevation: 10 degrees
- Propagation Parameters:**
 - Reference Date: day 21, month 3, year 2014
 - Elapsed time since 0h UT: hr 0, min 0, sec 0
 - Propagation Duration: 1 days
 - Propagation step: 60 sec
 - Perturbations: ☒ J2, ☐ Drag
- Calculations:**
 - ☐ RACE Radiometer Experiment
 - ☐ Downlink Data
 - Initial Charge: 100 %
 - Depth of Discharge: 50 %
 - Attitude Configuration: ☐ 1. Along-track, ☒ 2. Science, ☐ 3. Data Transmission
 - Spin Rate: 0 rpm
- Run:** A large button to execute the simulation.

Figure 4: *Graphical User Interface*

The first section labeled “Orbital Parameters” lets the user modify the parameters of

the orbit studied. A circular ISS-type orbit of altitude 420 km and inclination 52 degrees is entered as a default. On the right side of that same section, either the Mean anomaly or the True anomaly may be specified in degrees while the other parameter adjusts automatically.

Next, the “Ground Station Parameters” may be used to specify the location of the ground station used. The UT-Austin ground station is available as a default location with its GPS coordinates entered. The user may enter a different station by clicking on “Other” and entering the latitude, longitude and altitude of the station above mean sea level. The “minimum elevation” section may be used to specify the minimum elevation at which the spacecraft is visible from the ground station. This user-specified elevation value is used regardless of the azimuth. A more accurate model may be later applied to account for buildings present in the antenna’s field of view.

Furthermore, the Propagation Parameters section lets the user specify the reference date of orbit propagation as well as the time elapsed since 0h UT to a second precision. The default date is March 21st 2014 at 0h UT. Next, the propagation duration and integration step may be defined. Note that though a greater precision is achieved with lower values of propagation step size, this increases the calculation time. A step size of 1 minute is recommended for a few days of orbit propagation and should be used if the radiometer experiment is simulated. Moreover, perturbations such as J2 and Drag are available with J2 set as a default. Note that adding perturbations also increases the simulation time but may be used for more accurate results.

Finally the “Calculations” section allows the user to select a Radiometer Experiment calculation which is specific to the RACE spacecraft. If selected, the user may then input the initial battery charge and the depth of discharge of the battery. The “Downlink Data” option can be selected to simulate data transfers to the ground station rather than data acquisition. If the user does not wish to perform calculations for a particular RACE mission phase, he/she may specify the attitude of the spacecraft under the “Attitude Configuration” section, as well as specify the spin rate of the spacecraft about its long axis. The user may then press the *Run* button to execute the program.

On the other hand, an input function, shown in Figure 5, may also be used. Similarly to the GUI described above, the user can specify the orbital parameters, propagation settings, reference date, ground station, etc. The user input section is clearly delimited in the function and the rest of the document is not to be modified.

```

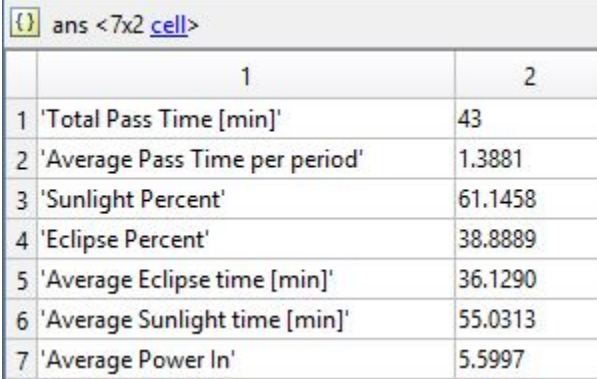
inputfunction.m x
20 %%%%%%%%%%%%%%%%%%%%%%%%%%%%%%%%%%%%%%%%%%%%%%%%%%%%%%%%%%%%%%%%%%%%%%%%%
21 %USER DEFINED INPUTS
22 |
23 %Satellite Orbit Parameters:
24 - ha = 420000; %apogee altitude in meters
25 - hp = 420000; %perigee altitude in meters
26 - inclination = 52; %orbit inclination in degrees
27 - w = 0; %argument of perigee in degrees
28 - Omega = 0; %Right Ascension of Ascending node in degrees
29 - M = 0; %Mean anomaly in degrees
30
31
32 %Propagation:
33 - duration = 1; %Duration of Orbit Propagation in days
34 - tstep = 60; %Integration step in seconds
35
36 %Define Reference date (date of propagation):
37 - day = 21;
38 - month = 3;
39 - year = 2014;
40 - t_initial = 0; %number of seconds elapsed since 0h UT of Reference date.
41
42
43 %Orbit Perturbations:
44 - optional = [1,0]; %[J2effect, drag] set entry to 1
45 %...to include those perturbations
46
47 %Define Ground Station Parameters
48 - wrw_latitude = 30.287559; %Latitude of WRW in degrees
49 - wrw_longitude = -97.73592; %Longitude of WRW in degrees
50 - wrw_h = 15; %height of WRW station in meters
51 - min_elevation = 7.5; %Minimum elevation in degrees
52
53
54
55 %Attitude Configuration
56 - attitude_config = 2; %Set to 1, 2, or 3 to determine attitude of spacecraft
57 %...(ignored for radiometer experiments).
58 - spin_rate = 0; %in rpm. (ignored for radiometer experiment).
59
60
61 %Radiometer Experiment Options
62 - dayradio = 0; %Set to 1 if want to simulate
63 %...radiometer experiment for RACE
64 - downlink_data = 0; %Set to 1 if want to simulate
65 %...data downlink for RACE
66 - DOD = 50; % depth of discharge in percent

```

Figure 5: *Input function example*

2.3 Program Outputs

This section describes the program outputs. The tool can be used to simulate a given orbit and yield a variety of useful information such as proportion of time spent in sunlight or the total time spent in view of the ground station. The default numerical outputs are shown in Figure 6. If the radiometer experiment is simulated, additional outputs will appear such as 'Average Power Out', 'Data Collection Duration' and 'Data Transfer Duration'.



ans <7x2 cell>	
	1 2
1	'Total Pass Time [min]' 43
2	'Average Pass Time per period' 1.3881
3	'Sunlight Percent' 61.1458
4	'Eclipse Percent' 38.8889
5	'Average Eclipse time [min]' 36.1290
6	'Average Sunlight time [min]' 55.0313
7	'Average Power In' 5.5997

Figure 6: *Standard Numerical Output Example*

In addition to numerical outputs, the program yields graphical outputs. The first is a groundtrack of the orbit with the ground station marked in red as shown in Figure 7.

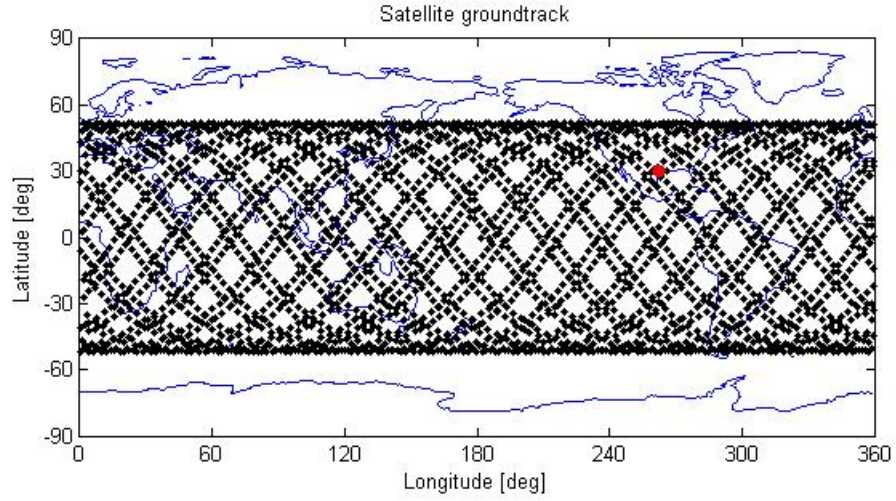


Figure 7: *Groundtrack Graphical Output Example*

Secondly, as shown in Figure 8, a 3D trajectory is constructed. The precession of the orbit due to J_2 is visible in that figure.

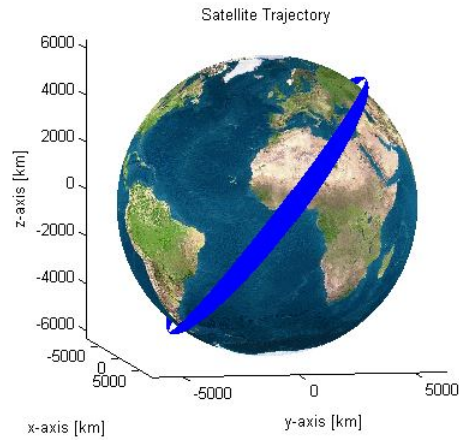


Figure 8: *3D Trajectory Graphical Output Example*

The program also outputs the power generated by the satellite, shown in Figure 9, over the duration of the trajectory. In this case, the calculation is performed for the RACE spacecraft. In the case of the simulation of the radiometer experiment, this graph includes

the power usage of the satellite vs. time.

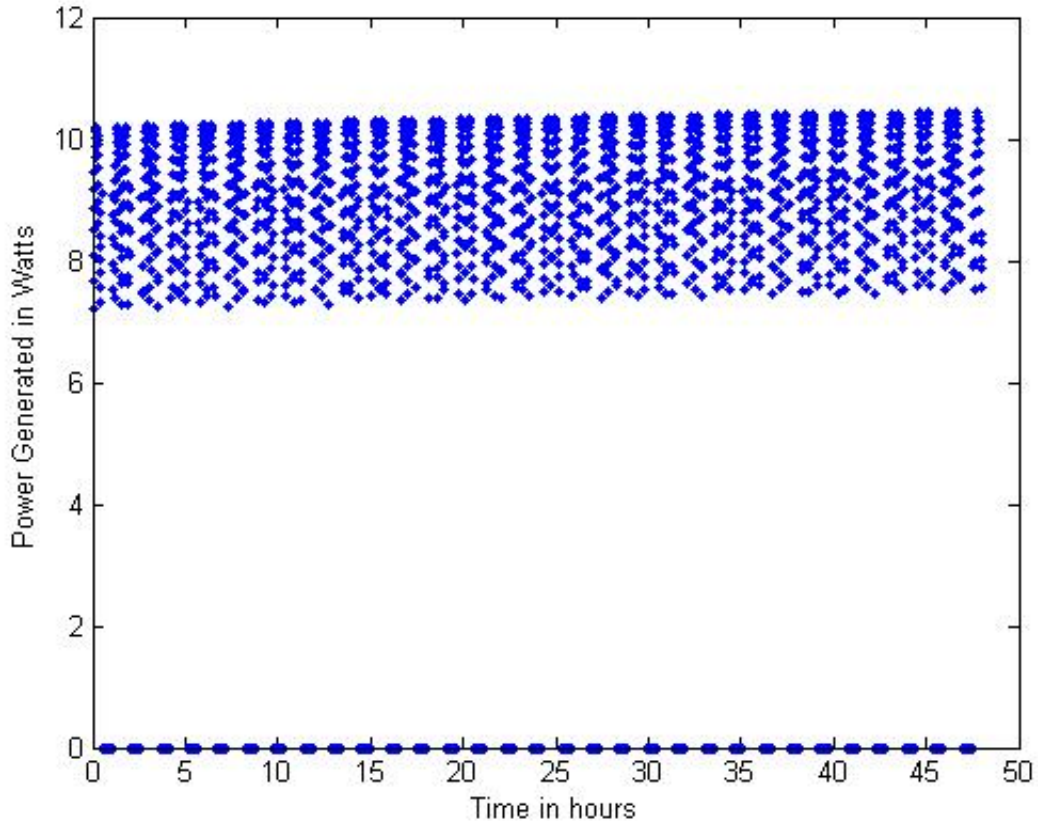


Figure 9: *Power Generated by Satellite Graphical Output Example*

Next, Figure 10 shows the power generation, the eclipse and sunlight periods and the ground station passes all on the same graph. This graph is particularly useful when analysing a specific mission phase.

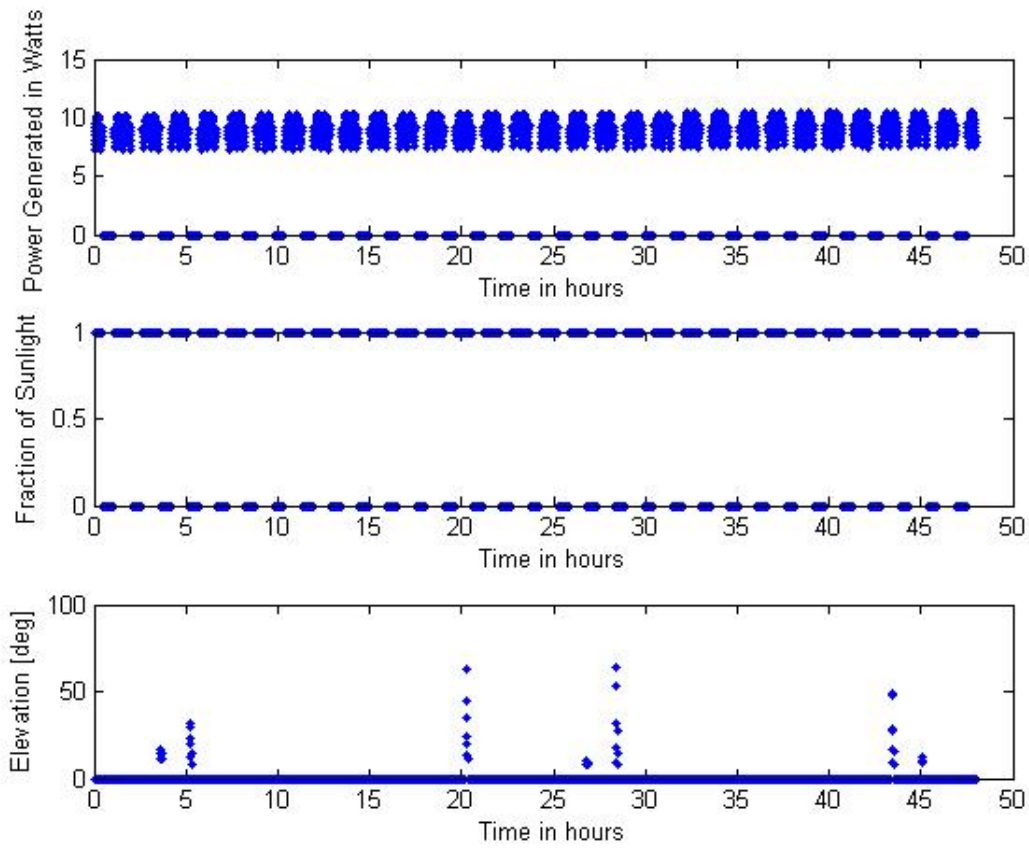


Figure 10: *Power Generated, Sunlight and Satellite Elevation Graphical Output Example*

Figure 11 further shows the ground station passes in more detail. Note that only the passes with elevation greater than the user-specified minimum elevation (in this case 7.5°) are shown in this graph.

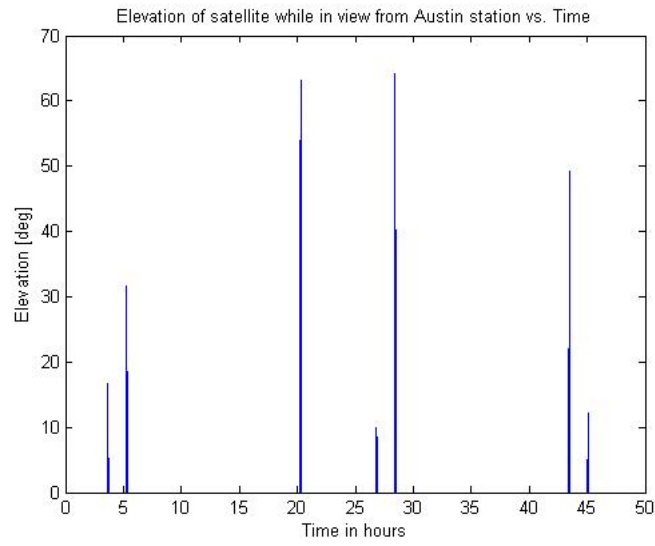


Figure 11: *Elevation of Satellite Graphical Output Example*

In Figure 12, the duration of each pass is graphed in a bar plot.

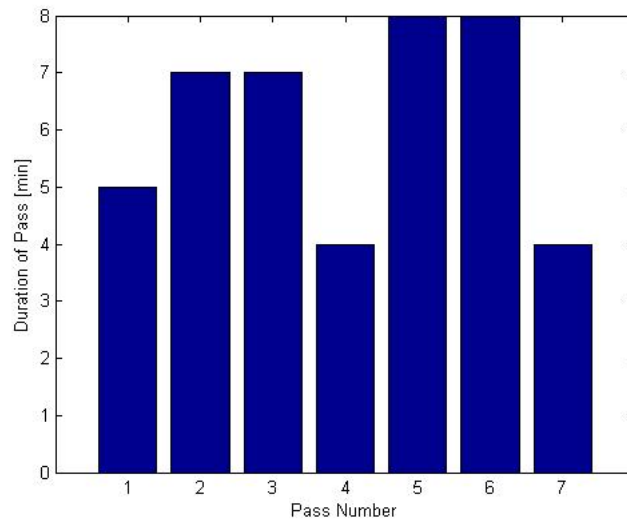


Figure 12: *Ground Pass Graphical Output Example*

Finally, the last graphical output shows the duration of each Sunlight and Eclipse period in minutes.

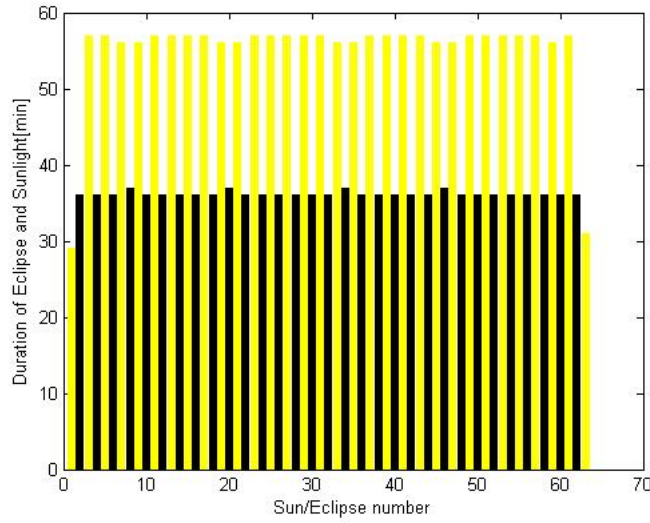


Figure 13: *Sunlight and Eclipse Graphical Output Example*

2.4 Orbit Propagation and Perturbations

As previously explained, the first phase of the program calculations is the orbit propagation. The orbit propagation is based on two body keplerian motion with optional additional perturbations. The orbit equations of motion are numerically integrated using MATLAB.

The user can choose to simulate the orbit using the regular central force model or include additional perturbations. The perturbations available are the J2 effect due to the Earth oblateness as well as the J3 and J4 effects. These perturbation effects are due to the Earth's nonspherical shape which causes variations in the gravitational potential [2].

Moreover, drag can also be included in the perturbations. The drag effect was determined using the U.S. Standard 1976 atmosphere model [8]. The atmosphere model data was linearly interpolated using an online MATLAB function included in the supporting functions in the 'bin' [9].

2.5 Satellite Geometry and Power generation

2.5.1 Sun Visibility

In order to determine the amount of power generated by the satellite at a given instant, the visibility of the Sun from the spacecraft has to be determined. The JPL SPICE toolkit provided the Sun ephemerides and a Matlab function was written to determine when the Sun is visible from the spacecraft, accounting for eclipse periods. Only the Earth was taken into account for Solar eclipses, disregarding other celestial bodies. The apparent solid angle of the Sun and Earth was calculated and their intersection determined. In order to determine if the Earth eclipses the Sun as viewed from the satellite, the apparent angular radius α_{Sun} and α_{Earth} of the Sun and Earth was calculated using the following equations [6]:

$$\alpha_{Sun} = \sin^{-1} \left(\frac{R_{sun}}{|\mathbf{r}_{sun}|} \right) \quad (1)$$

$$\alpha_{Earth} = \sin^{-1} \left(\frac{R_{earth}}{|\mathbf{r}_{earth}|} \right) \quad (2)$$

Where R_{sun} and R_{earth} are the actual Sun and Earth radii respectively and \mathbf{r}_{sun} and \mathbf{r}_{earth} are the Sun and Earth vectors from the satellite. The separation angle α between the two celestial bodies as viewed from the satellite is calculated using the four-quadrant inverse tangent:

$$\alpha = \tan^{-1} \left(\frac{\mathbf{r}_{sun} \times \mathbf{r}_{earth}}{\mathbf{r}_{sun} \cdot \mathbf{r}_{earth}} \right) \quad (3)$$

If the separation angle α between the Sun and the Earth is greater than their combined apparent angular radii, then there is no intersection :

$$\alpha \geq \alpha_{Sun} + \alpha_{Earth} \quad (4)$$

It is assumed that if the two conic sections intersect, the Sun is not visible from the spacecraft. This leaves a margin of error for power determination, with periods where the Sun is partially visible considered eclipse periods. Furthermore, these periods are usually very short (a few minutes) so they can be neglected.

2.5.2 Satellite Geometry and Attitude

A picture of the Radiometer Atmospheric CubeSat Experiment (RACE) satellite is shown in Figure 14. The satellite is a rectangular prism with 6 solar cells on each long side and 2 solar cells on each base. The body fixed axes \hat{x} and \hat{y} define the base of the prism while the \hat{z} axis is fixed to the prism long axis of symmetry. Each solar cell is a Spectrolab Ultra Triple Junction with 28.3% average efficiency with $135.3mW/cm$ as given by the manufacturer's specification sheet [10]. For $32cm^2$ solar cells, the maximum power of the solar cells is estimated to be 1.2 W.

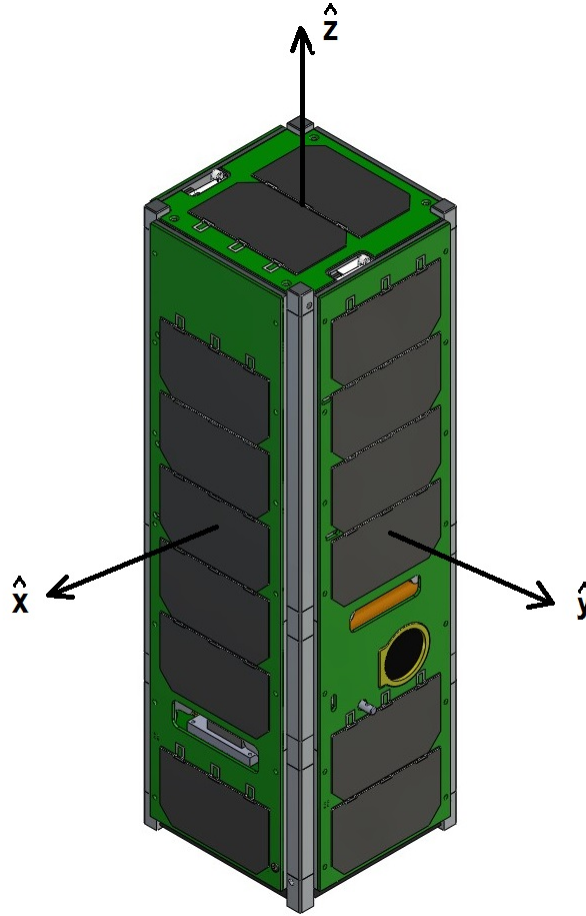


Figure 14: *RACE Drawing*

In order to determine how much power is generated by the satellite at a given instant, Lambert's cosine law was used. Lambert's law relates the irradiance of a surface to the

angle between the incident light rays and the surface normal:

$$I = I_0 \cdot \cos(\theta) \quad (5)$$

Where I is the surface irradiance in $W \cdot m^{-2}$, I_0 is the solar irradiance and θ is the incidence angle between the incoming light rays and surface normal direction. Consequently the power generated by the solar panels is reduced by a factor of $\cos(\theta)$ of the angle between the solar rays and the surface normal vector[7]. Using the Sun ephemeris and known satellite geometry, position and attitude at a given time, the angle between the Sun and each face of the satellite can be determined, and consequently the amount of power generated by the spacecraft at a given instant. Three power configurations were implemented and studied in the program. These attitudes of interest are the following:

1. \hat{z} axis pointed in the orbit along-track direction (parallel to the velocity vector);
2. \hat{z} axis perpendicular to the along-track direction and perpendicular to the satellite radius vector;
3. \hat{z} axis collinear with satellite radius vector.

These configurations are further illustrated in Figure 15. The first configuration can be used to reduce drag as the area normal to the velocity vector is minimized. The second configuration is used during the RACE spacecraft science mode, while the radiometer collects data. Finally the third configuration has the antennas of the spacecraft pointing towards the Earth which optimizes ground communication and facilitates data transfers.

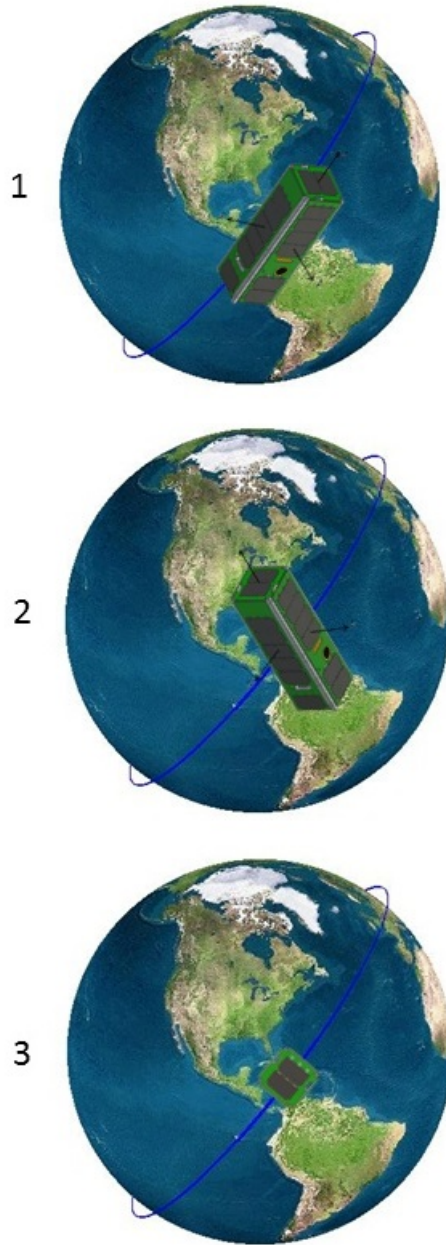


Figure 15: *Satellite Configurations*

For each of these attitudes, the initial configuration has the satellite's body axes parallel or perpendicular to the satellite radius vector. The RACE satellite has the further capability of spinning about its z axis.

3 RACE Mission

In order to demonstrate the capabilities of the Tool developed, the Radiometer Atmospheric CubeSat Experiment (RACE) mission was used as an example. This section describes the mission objectives, operations and the RACE power system.

3.1 RACE Mission Requirements and Radiometer Instrument

The RACE mission is the result of a collaboration between JPL and UT-Austin. The Texas Spacecraft Laboratory is responsible for the design and delivery of the CubeSat while JPL delivers the radiometer payload [11]. The RACE cubesat is a 3U CubeSat (10 cm x 10 cm x 30 cm) with the radiometer payload taking up half the volume of the satellite. The microwave radiometer payload will measure water vapor radiation at the 183 GHz line which is significant for Earth weather and precipitation studies [12]. In effect, the 183 GHz absorption line is highly sensitive to low amounts of precipitable water vapor which makes it ideal for studying and improving climate prediction [13]. A main mission objective is to demonstrate the technology of the radiometer by collecting 50 hours of science data over the course of the mission and transmitting the data to the UT-Austin ground station. The RACE mission will thus perform the spaceborne validation of the radiometer as well as provide atmospheric data.

The radiometer experiment phase of the mission will be ground-commanded and follow the spacecraft full system checkout and testing. The testing will target the attitude determination system to demonstrate its capability to control the spacecraft. The spacecraft will then enter its science mode which is dedicated to collecting data with the radiometer and transmitting it to the ground. This phase of the mission will be the focus of this tool's simulations.

Furthermore, the radiometer instrument imposes specific requirements to the spacecraft. While the radiometer is in operation, the spacecraft must spin at a constant rate. Additionally, the radiometer instrument can be operated in "Standby Mode", which means that the instrument is on, but does not collect data. This mode consumes about 1 Watt of power. Furthermore, the instrument's sensitivity requires it to warm up for 3 hours before starting to collect data if it was previously turned off. With the instrument in "Science Mode", the radiometer collects data and consumes about 1.3 Watts of power.

3.2 RACE Power System

The RACE spacecraft instruments include actuators, sensors and a flight computer for attitude determination and control, a command, data and handling computer, communication system including the radio and antenna and the power system in addition to the radiometer payload. The RACE power system is comprised of a 30 Watt-hr GomSpace battery with two regulated power buses of 3.3V and 5V [14]. When the spacecraft is power-positive, i.e there is more power consumed than generated, the batteries are charged. On the other hand, the batteries are discharged when the spacecraft is power-negative. When the spacecraft is in the shadow of the Earth and no power is generated by the solar cells, the power necessary to operate the spacecraft is provided exclusively by the battery. In order to simulate a safe battery operation, the battery should not be discharged entirely during the mission. The user may define the acceptable depth of discharge in the program which is set at 50% by default.

During the radiometer experiment, prior to the radiometer being turned on, the power draw from all subsystems with the radio not transmitting is of approximately 4.9 Watts. Once the radiometer is switched to standby mode, this power usage rises 5.8 Watts. When the data collection starts and the radiometer operates in science mode, the power rises to 6.2 Watts. Finally, while downlinking data with the radiometer on standby, the power consumption is at 9.1 Watts.

4 Validation

In order to verify the correctness and validity of the tool developed, a series of test cases were implemented and examined. The test results were then compared to results obtained from reliable sources. In this section, the overhead pass determination capability as well as the power generation was validated.

4.1 Overhead Passes

Firstly, the overhead pass determination capability of the program was examined. In order to verify the validity of the code written, the ISS orbit was modeled and the passes above a specified ground station were calculated. The data used for orbit propagation was taken from the Heavens Above website taking as a reference the ISS orbit on October 4th 2013. Heavens above yields reliable data for satellite passes above a user-specified ground station. The satellite orbit parameters used are the following, as given by Heavens Above, extracted from two-line orbital elements [4]:

Apogee height ha	Perigee height hp	Inclination i	Argument of Perigee ω	Right Ascension of Ascending Node Ω	Mean Anomaly M
420 km	417 km	51.6°	351.9545°	286.5472°	109.7717°

Table 2: Reference ISS orbit parameters [4]

The reference ground station used was the UT-Austin Aerospace Engineering building W.R. Woolrich (WRW) Laboratories located at latitude and longitude 30.29° N –97.74° E. The ground station height above sea level was taken to be 15 meters with a minimum elevation of 10°. A more accurate future value of the altitude for WRW would be closer to 150 meters, however this would be negligible in calculations. Figure 16 shows the groundtrack for this ISS orbit over one day starting on October 4th 2013 at 0h UT. The location of the UT-Austin ground station is also shown.

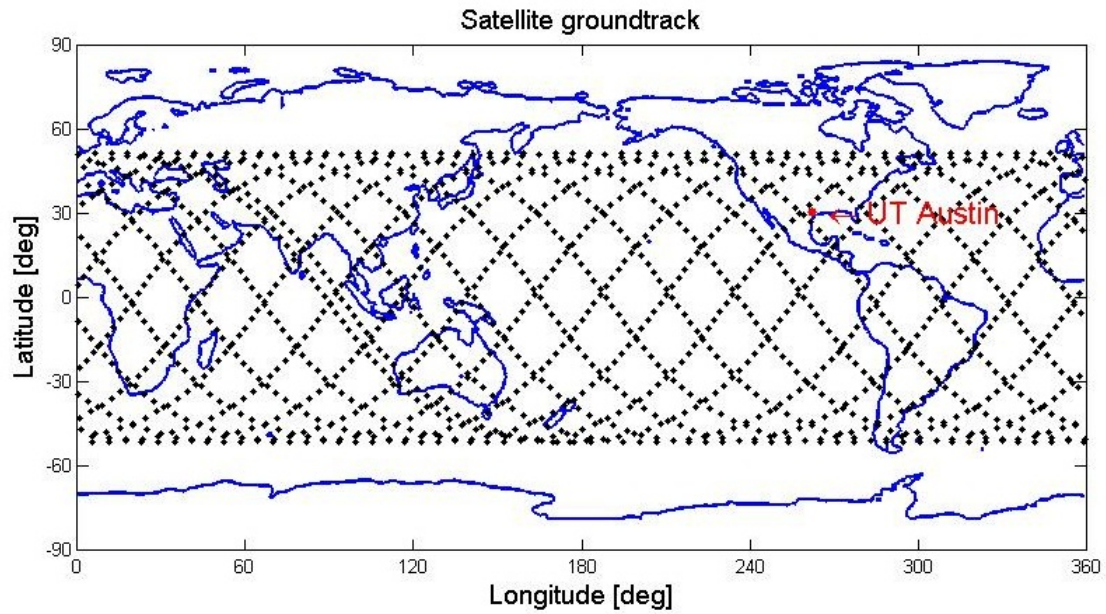


Figure 16: *ISS orbit groundtrack over 1 day*

Figure 17 shows an enlargement of the satellite groundtrack in the vicinity of the UT-Austin ground station. Figure 18 further portrays the visible passes as given by the Heavens Above website [4]. Comparing these two figures, the groundtrack of the passes seem consistent. There are two clear ground passes that come very close to the ground station in figure 17. A third less marked pass travelling north-west to south-east is corroborated by the Heavens Above graphs in Figure 18 .

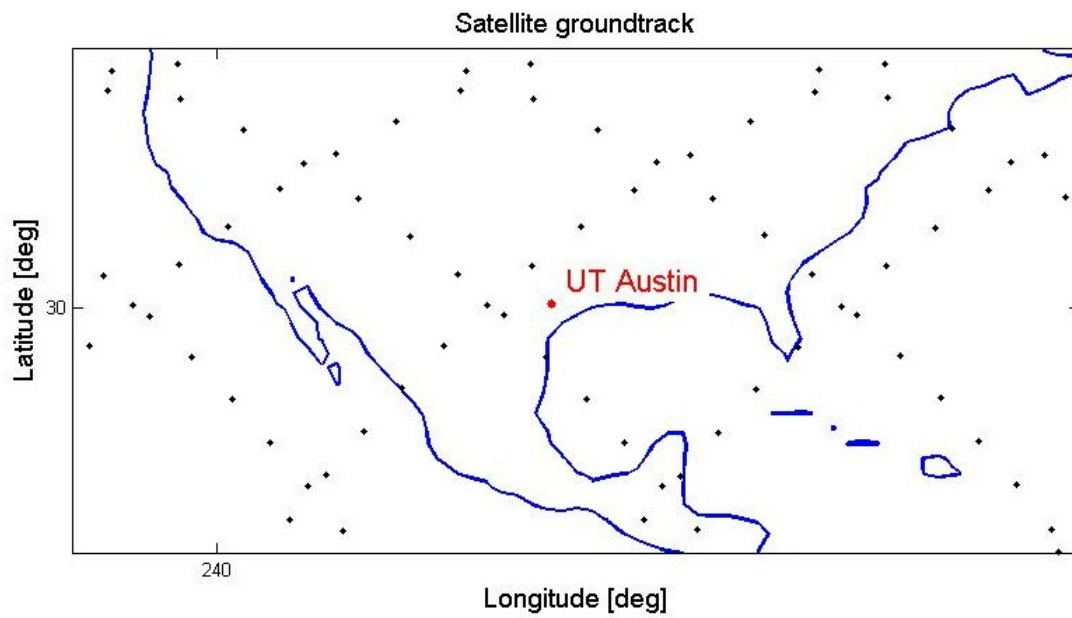
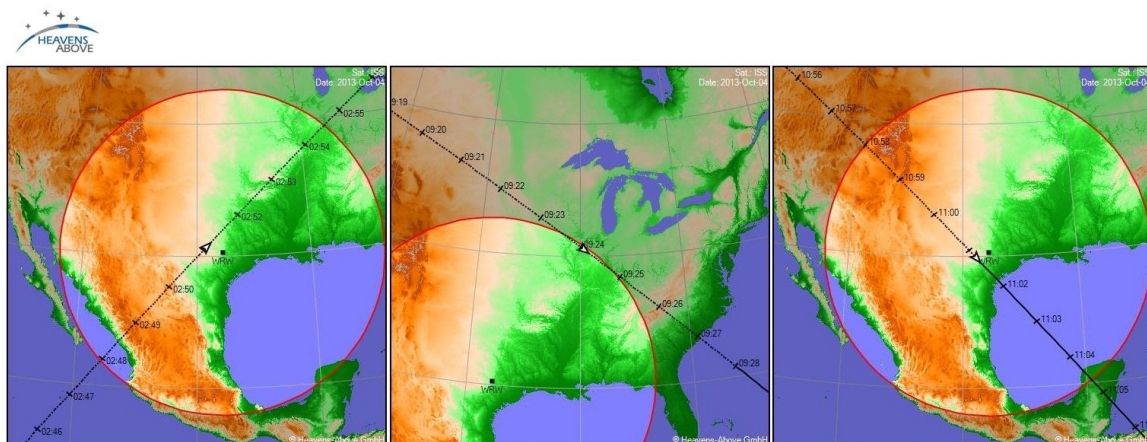


Figure 17: ISS orbit groundtrack over 1 day enlarged around Austin



In addition to the graphs previously shown, our tool and Heavens above yield the following data for the ISS passes. Note that for computation time purposes, the times given by the program are given with 1 min precision since the integration step is taken to be 60 seconds.

Program							
Pass #	t_{start}	Elevation	t_{max}	Elevation	t_{final}	Elevation	Duration
1	2:48	14°	2:51	52°	2:54	10°	6 min
2	9:23	11°	9:24	13°	9:25	12°	2 min
3	10:59	17°	11:01	50°	11:04	15°	5 min
Heavens Above [4]							
Pass #	t_{start}	Elevation	t_{max}	Elevation	t_{final}	Elevation	Duration
1	02:47:54	10°	2:51:13	70°	2:54:33	10°	5.5 min
2	9:23:31	10°	9:24:12	10°	9:24:53	10°	1.4 min
3	10:57:59	10°	11:01:20	76°	11:04:40	10°	6.7 min

Table 3: Satellite passes above UT-Austin on Oct 4th 2013

The results shown in Table 3 demonstrate that the passes predicted by our program are close to the passes predicted by Heavens Above. The start and end times of the passes do not differ by more than a minute while the maximum pass duration discrepancy is 1.7 minutes for the third pass. One should note that the programs yields satellite locations at one minute intervals. On the other hand, Heavens above yields its results with an order of second precision. This may explain the discrepancies in elevation and start and end times. Furthermore, only the J2 effect was taken into account in our simulation of the satellite orbit for this test and the Earth is assumed spherical. One can assume that a higher degree of accuracy could be achieved by accounting for additional perturbations and a more accurate Earth shape model. However for our purposes these results are more than adequate. One can therefore confidently conclude that the program accurately models satellite trajectories and overhead passes given a ground station and orbital parameters.

4.2 Power Generation and Attitude Validation

4.2.1 Static validation

In addition to validating the orbit propagation and pass time capabilities of the program, an important aspect to verify is the accurate attitude and power modeling. In order to validate this program capability, the satellite was placed in a series of strategic positions and attitudes by using a vernal equinox reference date (March 21st 2014 at 0hr UT). A vernal equinox reference date was used in order to position the Sun along the Earth Centered Inertial frame x-axis. Note that the reference for the ECI J2000 frame is the mean equator at equinox 2000 [5]. In 2014, one must keep in mind that the Sun will be slightly off the x-axis, but this discrepancy is very small.

4.2.2 ISS orbit with $\Omega = 0^\circ$

The satellite was first placed in an ISS type circular orbit with altitude 420 km, inclination 52° with right ascension of ascending node $\Omega = 0^\circ$ and Mean anomaly $M = 0^\circ$. In this position, the Earth-satellite and Earth-Sun vectors are essentially collinear. The satellite power generation was modeled in configuration 1, with the \hat{z} axis pointed in the orbit along-track direction and the \hat{x} axis along the satellite radius vector. At that instant, the \hat{z} and \hat{y} axes are virtually perpendicular to the Sun Vector while the \hat{x} axis points along the Sun vector. In effect, in that configuration, only one long face of the satellite should be in full Sun. Figure 19 shows the position of the satellite at that instant as well as the direction of the Sun.

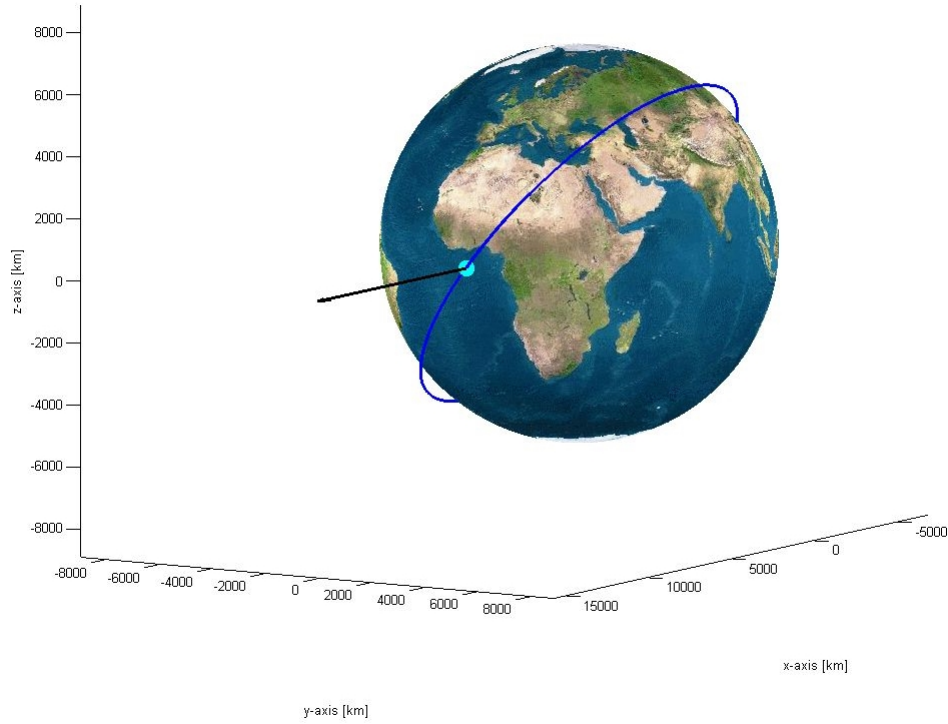


Figure 19: *Satellite position (light blue), orbit (dark blue) and Sun direction (black arrow)*

	\hat{x}	\hat{y}	\hat{z}
θ (degrees)	0.09563	89.95	89.92
Power Generated (Watt)	7.200	0.0058	0.0035
Total Power Generated (Watt)	7.209		

Table 4: Power generated with one large face in full sun

Table 4 lists the power generated by the satellite in the given configuration. The first line yields the angle between the axis direction and the Sun direction while the second line yields the power generated by the surfaces perpendicular to each axis. As expected, the power is almost entirely generated by the long face in full view of the Sun. Since there are six solar panels on that face and the angle of the surface normal to the Sun is close to null, each solar cell yields the maximum power of 1.2 Watts. As expected, the total power generated is approximately 7.2 Watts.

4.2.3 ISS orbit with $\Omega = 180^\circ$

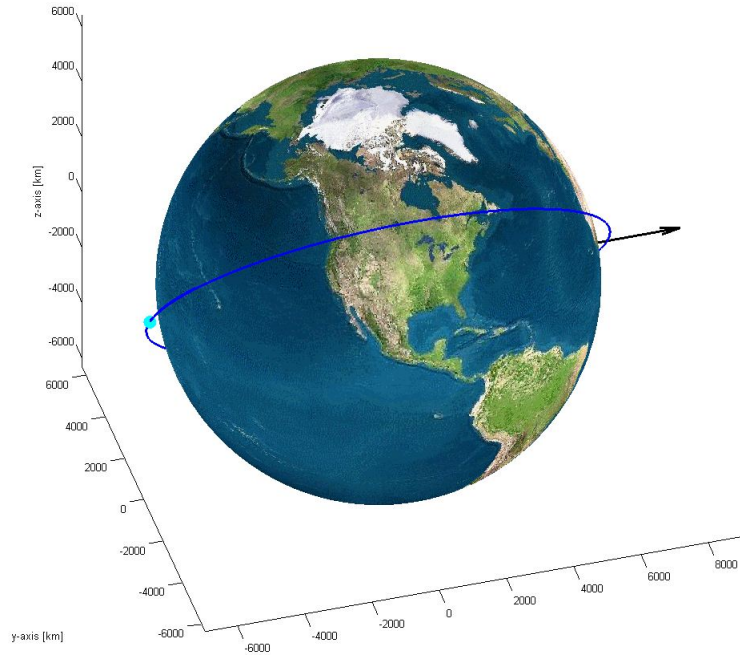


Figure 20: *Satellite position (light blue), orbit (dark blue) and Sun direction (black arrow)*

The same ISS orbit was modeled with Ω taken to be 180° in this case. This places the satellite in the shadow of the Earth, in the opposite direction of the Sun shown in Figure 20. In this case the program calculates that no power is generated by the satellite since it is located in the shadow of the Earth.

4.2.4 Equatorial orbit with $\Omega = 90^\circ$

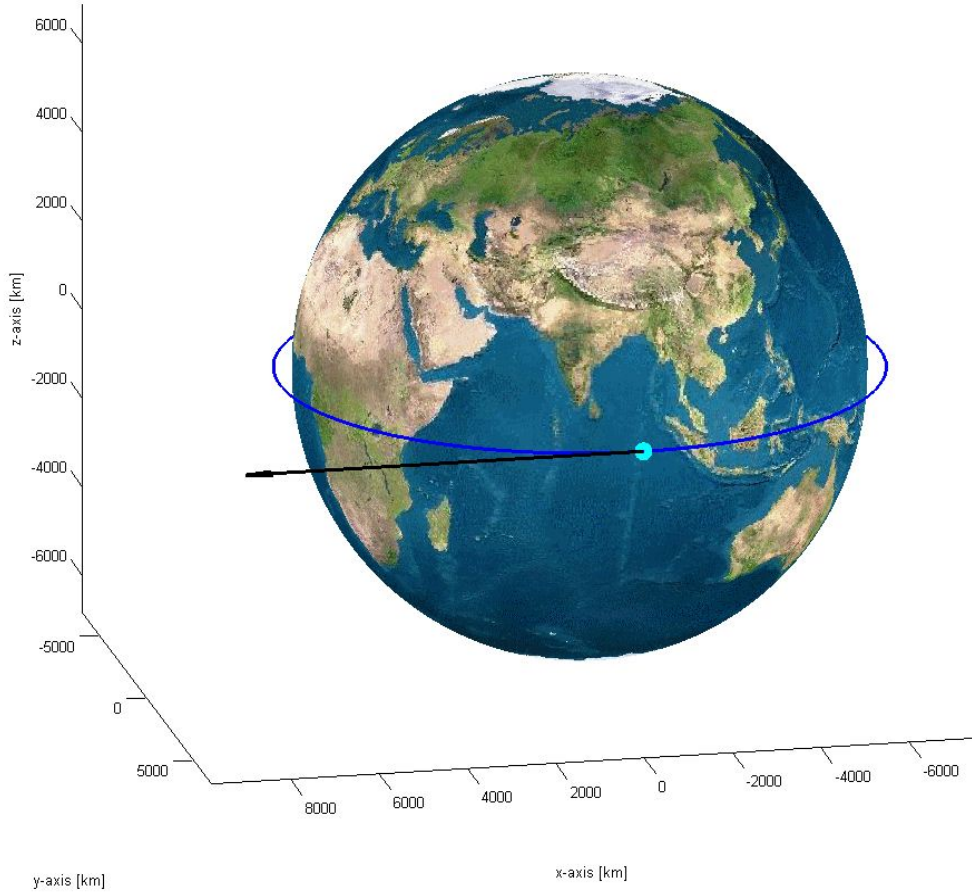


Figure 21: *Satellite position (light blue), orbit (dark blue) and Sun direction (black arrow)*

The next orbit simulated is an equatorial orbit with inclination $i = 0^\circ$ shown in Figure 21. In this position, one small face of the satellite should be in full Sun, as demonstrated in Table 5. Since only one small face is in full Sun and two solar panels are located on the small face, the satellite generates approximately 2.4 Watts in this given position.

	\hat{x}	\hat{y}	\hat{z}
θ (degrees)	89.91	89.96	0.09356
Power Generated (Watt)	0.011	0.0048	2.400
Total Power Generated (Watt)	2.415		

Table 5: Power generated with one small face in full sun

4.2.5 ISS orbit with $\Omega = 90^\circ$

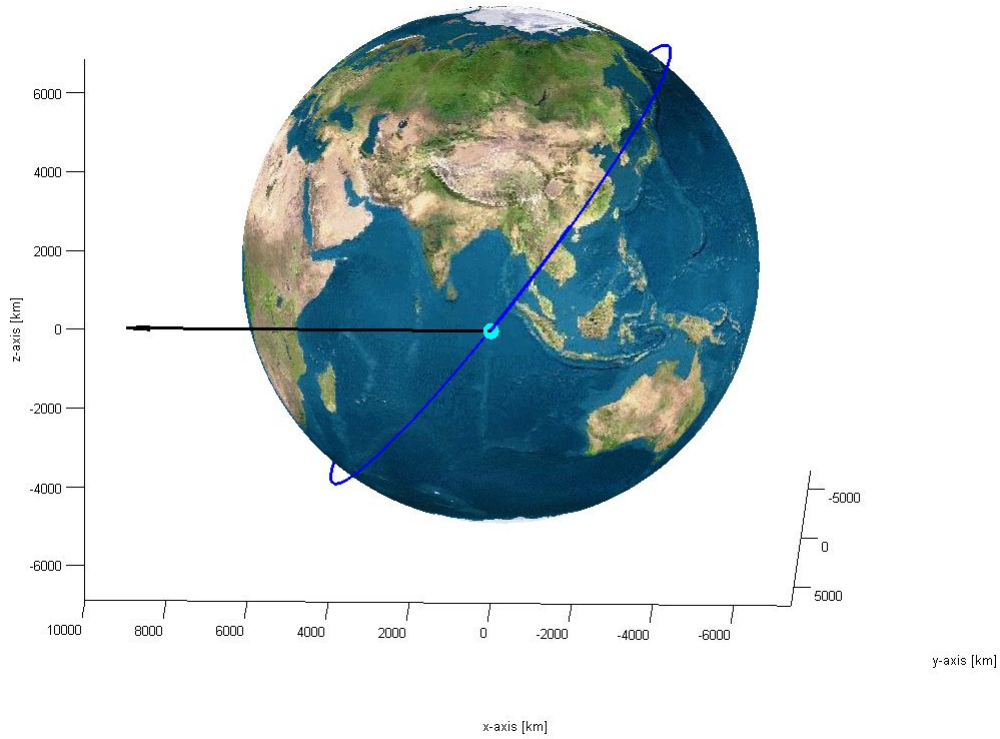


Figure 22: Satellite position (light blue), orbit (dark blue) and Sun direction (black arrow)

Finally, the satellite was placed in an ISS orbit with $\Omega = 90^\circ$ with its \hat{z} axis along the velocity vector. In this case, both a long face and a small base of the satellite are exposed to the Sun, though not at a right angle, as shown in Table 6. Since both the θ_y and θ_z angles are greater than 90° , this means that the opposite corresponding face is receiving sunlight. Indeed, due to the symmetry of the spacecraft, only one of a given pair of parallel satellite

faces can receive sunlight at a given time.

	\hat{x}	\hat{y}	\hat{z}
θ (degrees)	89.91	142.0	128.0
Power Generated (Watt)	0.011	5.677	1.476
Total Power Generated (Watt)	7.164		

Table 6: Power generated with two faces exposed to sunlight

From the previous static power simulation tests, it can be concluded that the program's satellite power generation is valid.

4.2.6 Dynamic Power Generation

As previously mentioned, although the program is capable of performing simulations with 1 second time interval integration steps, this is very time consuming. In the interest of speeding up simulations, most are performed with 1 minute time steps. In this section, the dynamic power simulation was studied in order to determine whether sampling the power generation every minute yields an accurate average value over the whole time interval. Indeed, this matter is of great significance as in certain situations, the spacecraft may be spinning while orbiting the Earth. The power generation would then constantly vary as faces are exposed to the Sun rays with different angles of incidence.

In the case of the RACE spacecraft, in experiment mode, the satellite is spinning at a rate of 6 rpm. Consequently, the spacecraft undergoes an integer number of revolutions every minute and essentially is in the same configuration every time the power sampling is performed. Thus, the program yields no power difference for a rotating spacecraft as a static one.

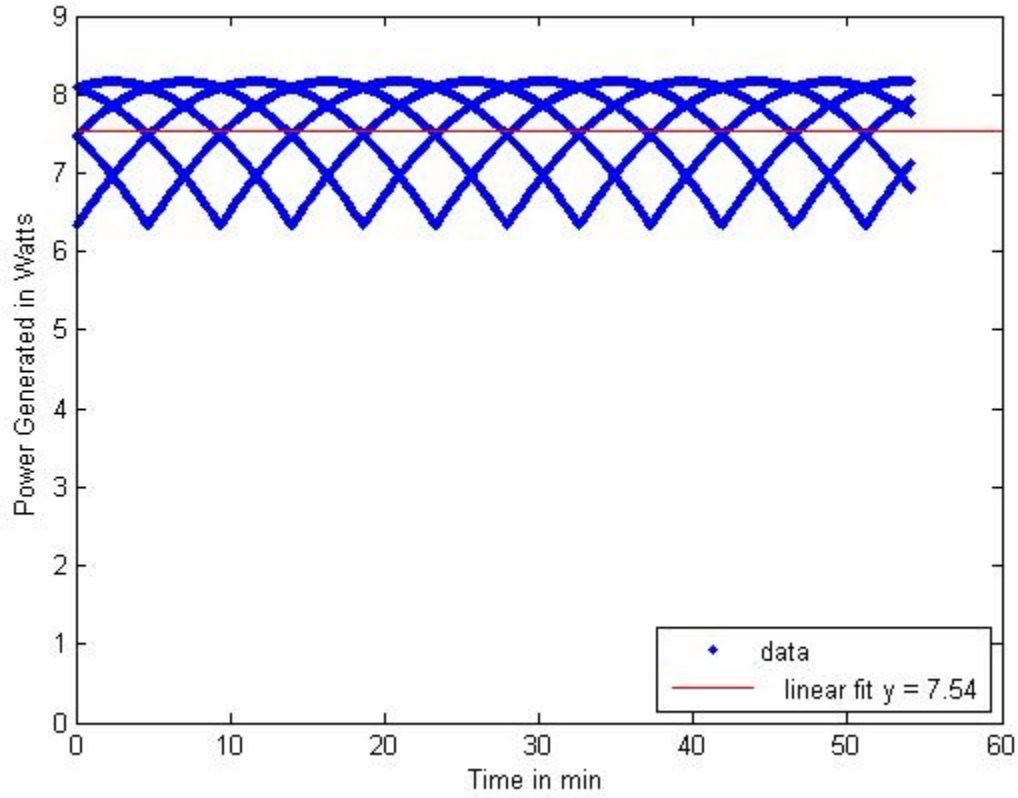


Figure 23: *Power generated over one hour sampling each second with linear fit*

An ISS type orbit was simulated with an $\Omega = 270^\circ$ starting on March 21st 2014 at 0h UT, sampling every second and every minute. Figure 23 shows the power generated over one hour, sampling every second. A linear fit was performed which yields an average value of 7.54 W.

Figure 24 shows the power generation for the same orbit over one hour, sampling every minute. A linear fit in this case yields an average value of 7.51 W. This is slightly lower than the average value of 7.54 W obtained by sampling every second. Repeating the simulations with various orbits at different times further shows that the discrepancy between 1 second time step and 60 seconds does not exceed 0.2 Watts.

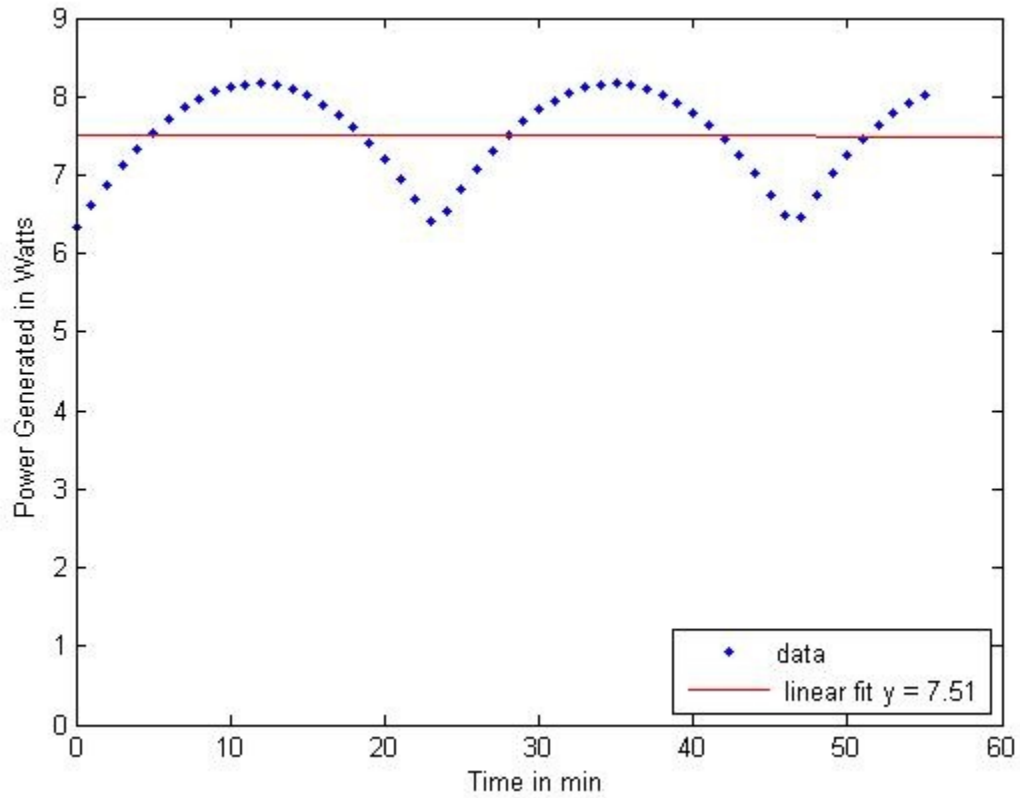


Figure 24: *Power generated over one hour sampling each minute with fit*

Figure 25 shows the average power generated by the spacecraft vs. Right Ascension of Ascending node computed using 1 min step size and 1 second step size. The 1 min average values were averaged over 2 days including eclipse times while the 1 second values were averaged over half a day for computation purposes. The values computed are fairly close and follow the same trend.

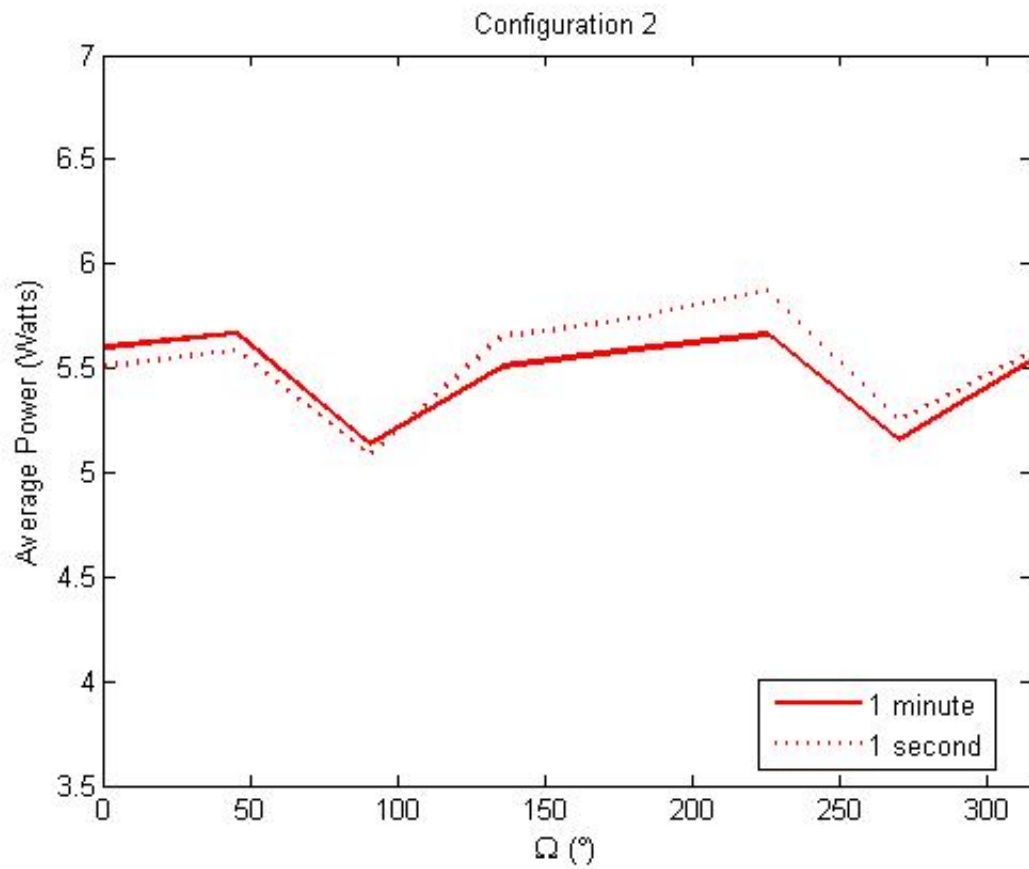


Figure 25: *Average Power Generated in Configuration 2 vs. RAAN*

We can thus conclude that sampling the power every minute yields fairly close results and is sufficiently accurate for simulation purposes. If desired, a higher degree of accuracy may be achieved at the expense of a longer computation time.

5 Results and Discussion

5.1 Sunlight

In order to determine the amount of sunlight received in orbit by the satellite at different moments of its lifetime, different orbit planes were studied. A reference date of March 21st 2014 was used in order to place the satellite plane strategically with respect to the known Earth-Sun vector. On that date, the Sun is approximately located along the vernal equinox direction, which is the reference x-axis in the Earth-Centered Inertial frame. An ISS type circular orbit of altitude 420 km and inclination 52 degrees was modeled with Right Ascension of Ascending Node Ω varying from 0 to 315 degrees. The orbit was propagated for 2 full days while accounting for J2 perturbation. The following table shows the percentage of sunlight and eclipse of those 2 day long trajectories :

$\Omega(^{\circ})$	0	45	90	135	180	225	270	315
<i>%Sunlight</i>	61.1	62.9	68.5	64.2	61.0	62.8	68.1	64.1
<i>%Eclipse</i>	38.9	37.1	31.5	35.8	39.0	37.2	31.9	35.9

Table 7: Sunlight vs. Orbit Right Ascension Ω

From Table 7, we can deduce that the satellite will receive more sunlight when in an orbit with Right Ascension 90° or 270° . That is, when the Earth-Sun vector is essentially perpendicular to the orbit line of nodes. Comparing this to the amount of time spent in sunlight for an orbit of Right Ascension 0° , the time spent in the Sun is increased by approximately 7% of the total trajectory time.

The average power generated at a given instant for these orbits was then determined, averaged over the two days. One may expect the orbits with a greater percentage of sunlight to yield the highest average power, however, this is not necessarily the case. Table 8 shows the average power generated for different cases for each configuration shown in Figure 15. These results are further graphed in Figure 26. Note that the eclipse times which yield no power were included in the calculation of the average.

$\Omega(^{\circ})$	0	45	90	135	180	225	270	315
1. $P_{av}(W)$	3.7844	5.3345	6.2621	5.6837	3.8067	5.2972	6.2184	5.6636
2. $P_{av}(W)$	5.5997	5.665	5.1339	5.5071	5.5914	5.6640	5.1530	5.5323
3. $P_{av}(W)$	4.2066	5.7445	6.6237	6.0846	4.2343	5.7122	6.5833	6.0628

Table 8: Average Power vs. Orbit Right Ascension Ω for each configuration

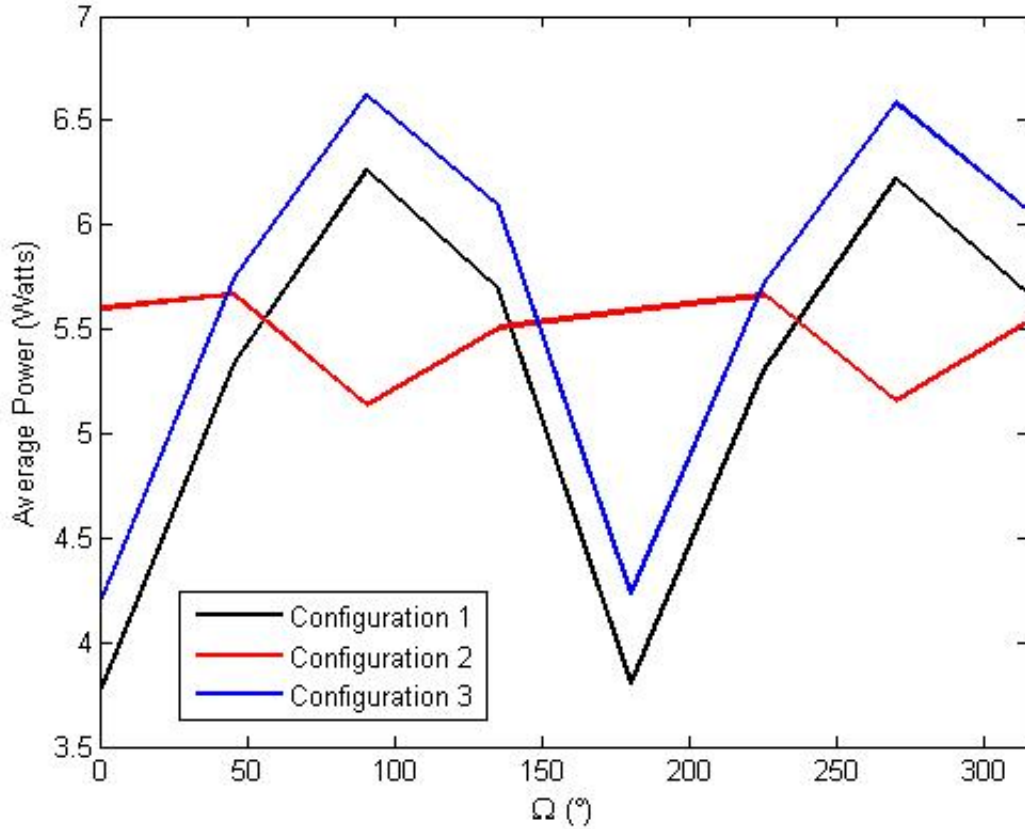


Figure 26: Average Power vs. RAAN for each Configuration

Although orbits with $\Omega = 90^{\circ}$ and $\Omega = 270^{\circ}$ receive approximately 7% more sunlight time than orbits with $\Omega = 0^{\circ}$, in configuration 2, $\Omega = 0^{\circ}$ yield a higher average power. On the other hand, in configuration 1, with the satellite \hat{z} axis along the velocity vector, $\Omega = 90^{\circ}$ and $\Omega = 270^{\circ}$ yield around 6.2 W on average while $\Omega = 0^{\circ}$ yields the lowest

average power value of the table at 3.8 W. This can be explained by the fact that when the satellite is in configuration 1 with $\Omega = 90^\circ$, the satellite in its orbit spends more time, not only in the sunlight, but with its long sides to the Sun. Since there are 6 solar panels on each long side, more power is generated when these are facing the Sun.

Moreover, this additional sunlight time before entering or after exiting an eclipse zone is spent with a great portion of its long sides in the Sun, fully taking advantage of the additional sunlight. On the other hand for $\Omega = 0^\circ$, not only is the sunlight time reduced, but the satellite spends most of its time with the short base oriented toward the Sun. When the satellite is above the equator, the Sun facing small base is tilted down, while when it is below the equator it is tilted up. Therefore, away from the equator, the small base is in full Sun while the Satellite-Sun vector is close to perpendicular to the long side surface normals. Since the solar radiation follows a cosine law, the power in those regions is greatly reduced.

On the other hand, in configuration 2, there are relatively lower discrepancies in average power generation from one Right Ascension to another. The power generation ranges from approximately 5.1 W (for $\Omega = 90^\circ$) to 5.7 W (for $\Omega = 45^\circ$). In this situation, the satellite with $\Omega = 0^\circ$ generates more power than $\Omega = 90^\circ$. In this configuration the satellite's larger faces receive more Sun when $\Omega = 0^\circ$ while the small face is more exposed to the Sun when the orbit plane is "normal" to the Satellite-Sun vector, undermining the power benefit of the longer sunlight time.

Consequently, in order to maximize power generation, not only does one have to examine the eclipse duration but, more importantly, the orbit plane orientation with respect to the Sun for different configurations. If the satellite is in an orbit whose line of nodes is close to parallel to the Earth-Sun vector, it would be advantageous for the satellite to be in configuration 2. On the other hand, for an orbit plane whose line of nodes is close to perpendicular to the Earth-Sun vector, the satellite would generate more power in configurations 1 or 3.

5.2 Radiometer Experiment

There exists a phase in the RACE spacecraft mission of particular interest, the radiometer experiment. An objective of the RACE mission is for the radiometer to collect 50 hours of data. In order to meet this requirement, it is important to understand and determine how many hours of data can be collected consecutively during a science experiment day. Knowing how much data can be collected before running out of power can then help adequately plan and improve mission operations. In the following simulations, a day in the life of the radiometer experiment for different orbits was studied, accounting for the power generated, the power draw from all systems and ground station passes.

5.2.1 Radiometer Experiment Data Collection

The scenario assumed for the spacecraft operations during this mission phase is the following, assuming the spacecraft transfers to science experiment for the first time.

1. The spacecraft is in configuration 3 in low power mode and waits for a ground pass.
2. A pass occurs and the spacecraft receives a command to start the scientific experiment. The spacecraft transitions to science attitude (configuration 2) and starts spinning.
3. The spacecraft takes approximately 450 minutes to achieve a constant spin, then waits for another ground pass.
4. A pass occurs, the spacecraft downlinks confirmation of stable spin rate and powers on the radiometer
5. The radiometer takes 3 hours to warm up in stand by mode.
6. Data collection begins and terminates when the battery reaches the user-determined depth of discharge .

Throughout the rest of the mission the spacecraft will maintain constant spin and repeat data collection. Only steps 4-6 will then be performed in subsequent data acquisition phases. In this simple scenario, at the beginning of the simulation, the battery is charged and subsequently discharged until it is at a 50% depth of discharge. In practice, the spacecraft would then enter a low power mode before discharging the battery entirely.

This scenario was applied to orbits of different Right Ascension of Ascending Nodes, starting at the same reference date of March 21st 2014 at 0h UT.

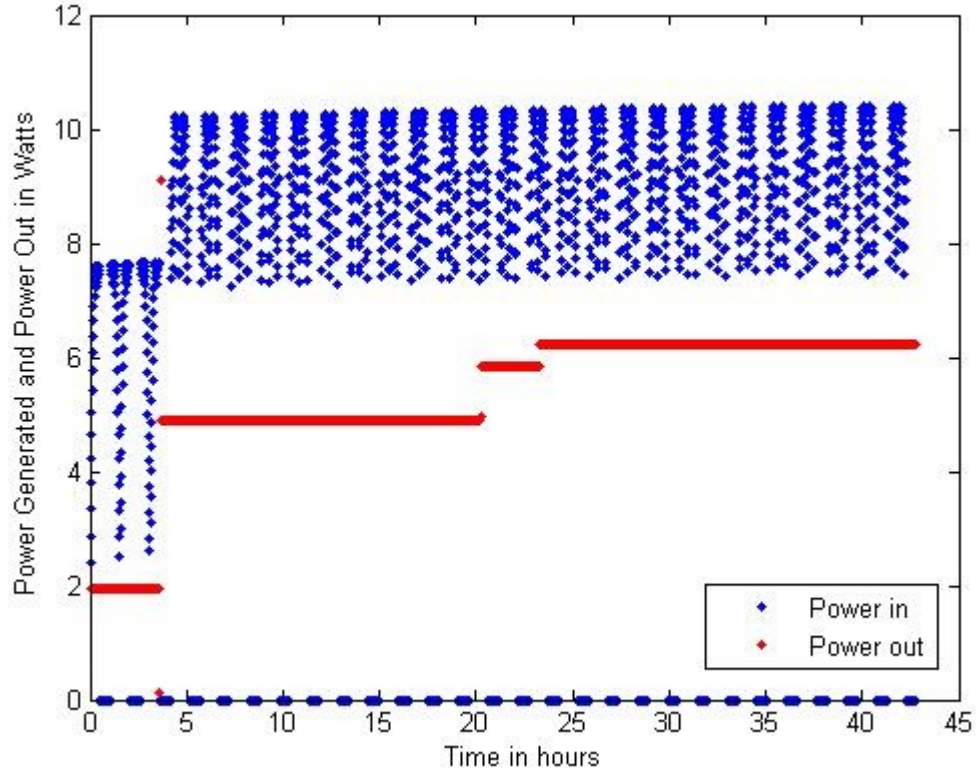


Figure 27: *RACE power during radiometer experiment with $\Omega = 0^\circ$*

Figure 27 shows the power generated by the spacecraft and the power used throughout the length of the experiment until the battery reaches 50% charge. Recall that although the instantaneous power generation sometimes exceeds 10 Watts, the eclipse times yield no power, resulting in power averages consistent with Table 8. Since the spacecraft starts in configuration 3 with $\Omega = 0^\circ$, from section 5.1, we have an average power generation of approximately 4.2 W which is relatively low. In the first part of the experiment, since the satellite is in low power mode, it expends 1.9 W which is lower than the average power generated in that first phase. The satellite therefore starts in a power positive state. Figure 28 shows the state of the battery with time during the experiment. It is visible that during the first phase, the satellite battery is fully charged while it waits for a ground pass.

After 3.6 hours, a ground pass occurs and the spacecraft transfers to configuration 2 and starts spinning. The power use in that configuration increases to 4.9W as noticeable on

Figure 27 around 5 hours. Looking back at Table 8 we can verify that the average power generated in configuration 2 with $\Omega = 0^\circ$ is around 5.6 W. Therefore, the spacecraft is still power positive in that phase and the battery remains charged over the time it takes to achieve constant spin. The satellite then waits until a new ground pass occurs to confirm stable spin rate which takes around 9 hours during which the battery remains fully charged.

Once a pass occurs, the radiometer is turned on and warms up for 3 hours before starting to collect data. The radiometer is set to standby mode in order to save power during the warm up time. The power consumption thus rises to 5.83 W which is visible in Figure 27 around 21 hours. The satellite in that phase is no longer power positive. Indeed, this is noticed in Figure 28 since around 21 hours, the battery charge begins to decrease. The radiometer then is put in data collection mode, with a power consumption rising to 6.19 W for the satellite. The satellite is thus slightly more power negative and achieves approximately 19.5 hours of continuous data collection before reaching 50% battery charge. Note that the same experiment with the radiometer turned fully on during warm up yields approximately 18.0 hours of data, ie. 1.5 hours less than with the radiometer in standby mode during warm up.

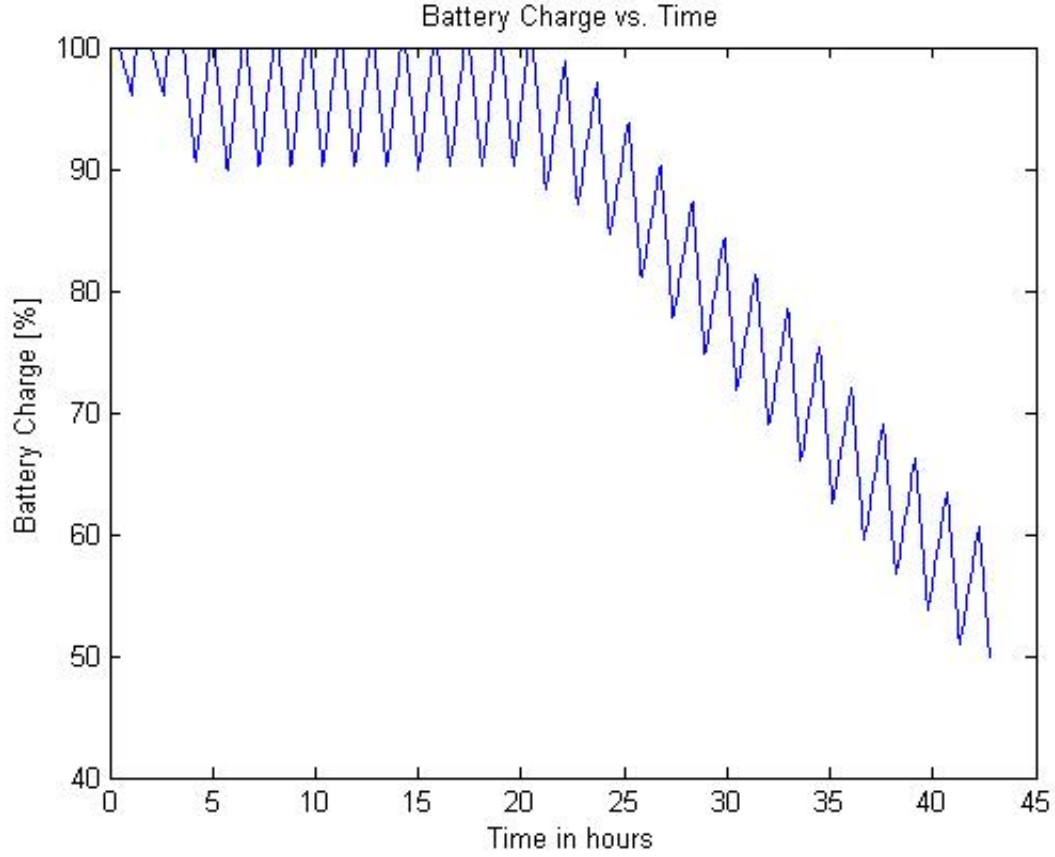


Figure 28: *Evolution of Battery Charge during Radiometer Experiment with $\Omega = 0^\circ$*

In the previous situation, the satellite was assumed to be fully charged at the beginning of the simulation. It is of interest to investigate how the operations may change if the satellite is, for example, only 70% charged. In this case, the satellite has enough time to recharge in low power mode while waiting for a ground pass as seen in Figure 29 from the steep positive slope from 0 to approximately 6 hours. The battery is thus fully charged prior to the radiometer being turned on and the same amount of data can be collected.

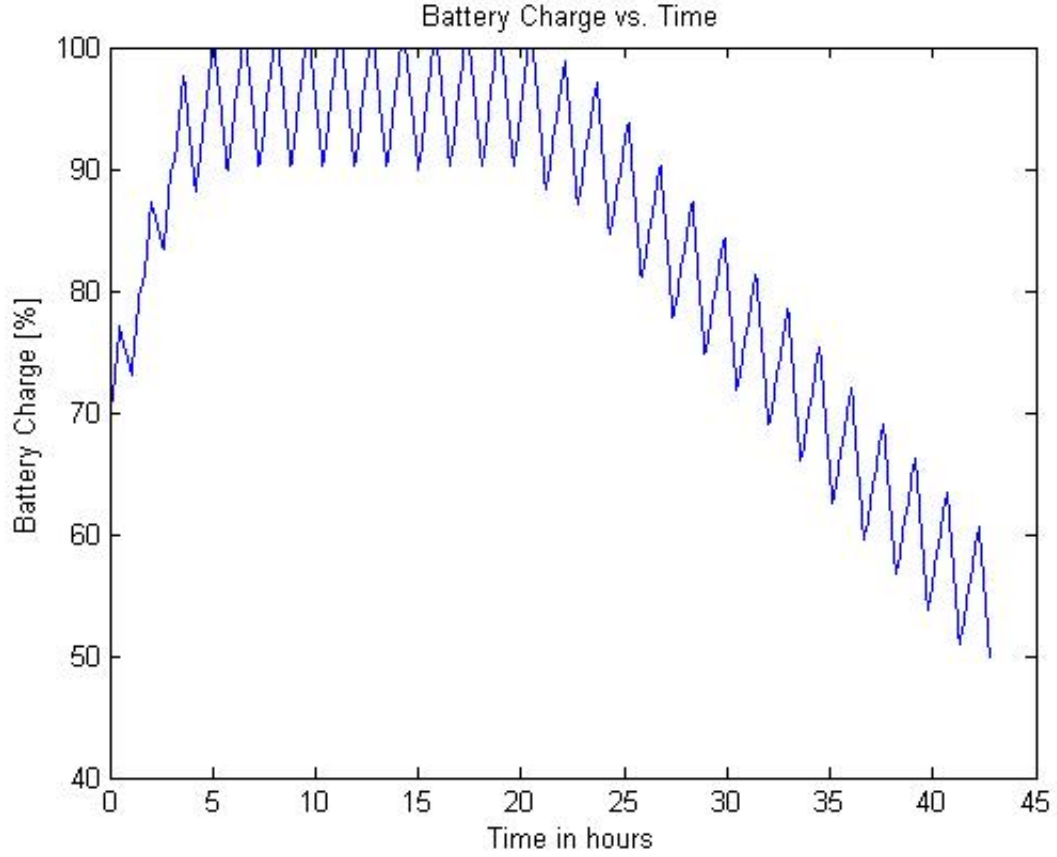


Figure 29: *Battery Charge vs. Time with $\Omega = 0^\circ$ (70% initial charge)*

The previous orbit studied with $\Omega = 0^\circ$ has a relatively high average power generation of 5.6 W in configuration 2 . That example would thus qualify as one of the best case scenarios for the radiometer experiment. In an orbit with $\Omega = 90^\circ$, the average power generation in configuration 2 is approximately 5.1 W (see Table 8). On the other hand, this orbit achieves the highest power generation in configuration 1. The radiometer experiment was thus simulated for this new orbit with an initial battery charged at 70% (see Figure 30).

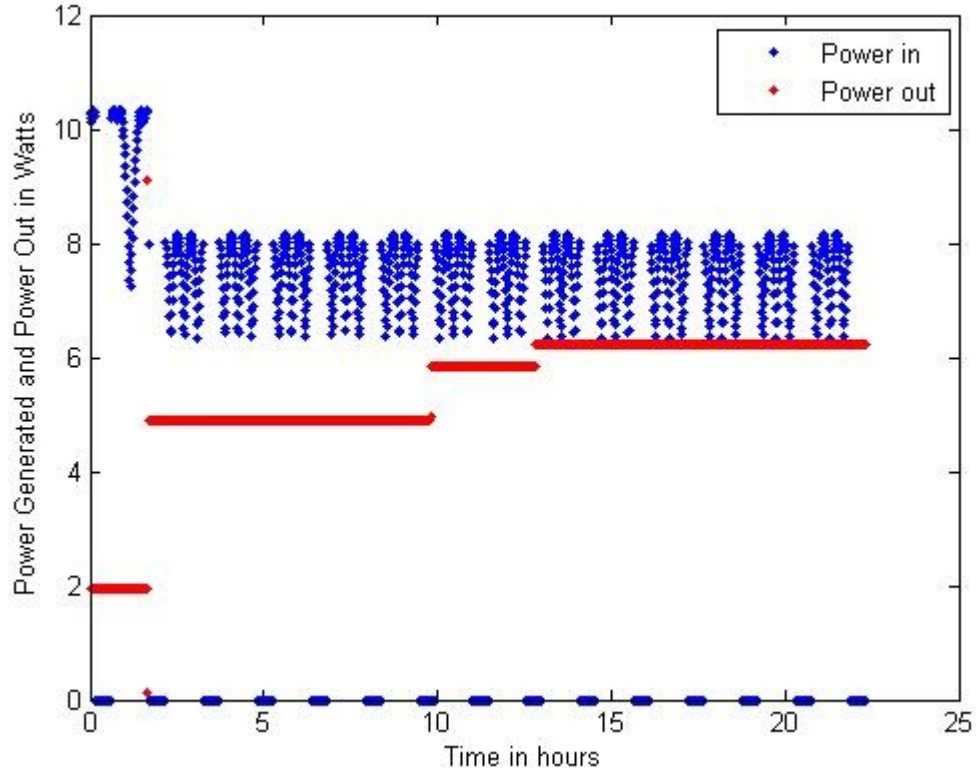


Figure 30: *RACE power during radiometer experiment with $\Omega = 90^\circ$*

Figure 30 shows that the power generation is high in the first phase of the experiment (from 0 to 1.65 hours) then drops to a lower value of approximately 5.1 Watts once the satellite has been changed to configuration 2. The satellite battery starts out with a 70% charge and gets almost charged fully during the 1.65 hours it waits for a ground pass and achieves 100% charge while in spin mode. Indeed the satellite remains slightly power positive while spinning in this orbit. After warming up the radiometer for the required time, it has to wait another 0.6 hours for another pass which is much less than in the previous example.

The satellite's battery is once again fully charged as the radiometer is turned on as shown around 9.5 hours in Figure 31. In this case, the radiometer achieves 9.5 hours of data collection which is less than half of the data collection time with the previous “good scenario”.

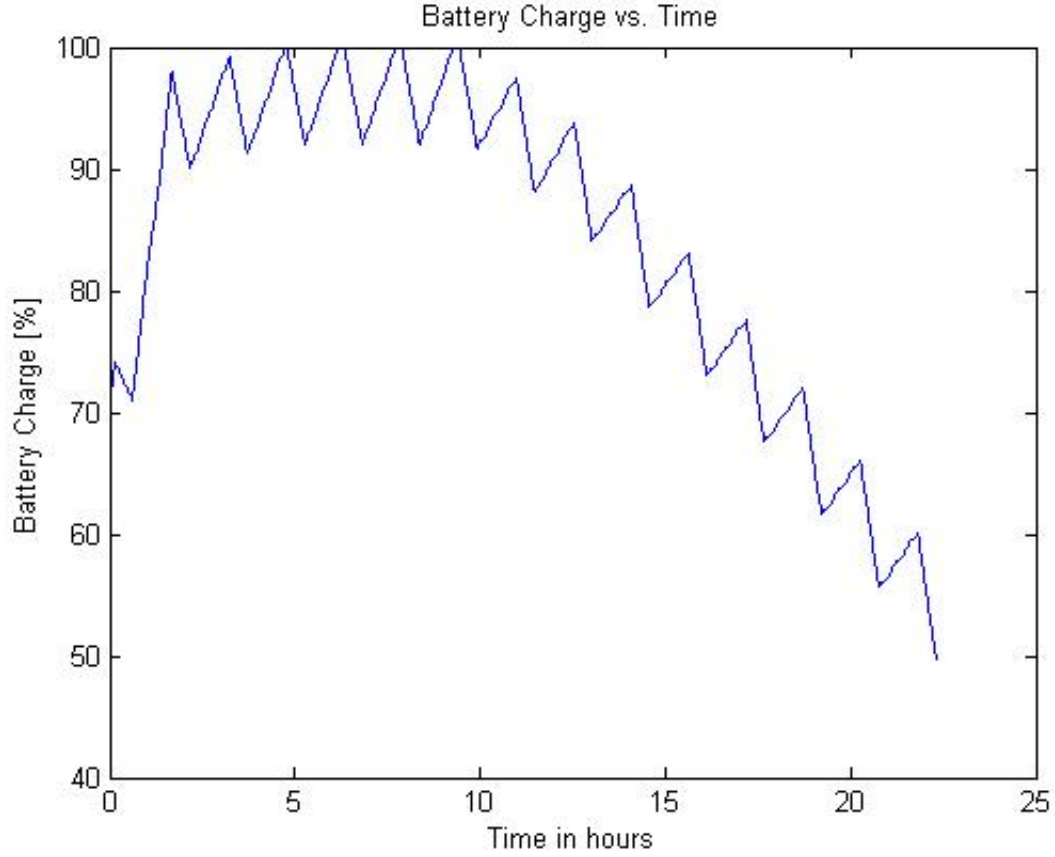


Figure 31: *Battery Charge vs. Time with $\Omega = 90^\circ$ (70% initial charge)*

In both the previous cases, since the satellite spends time in low power mode before the satellite is transitioned to science mode and spins, the satellite has the time to fully charge before starting the experiment. In the following experiment, the satellite is in the same orbit with $\Omega = 90^\circ$, however, the satellite almost immediately passes over the ground station which commands it to start spinning. It consequently does not have time to recharge in low power mode.

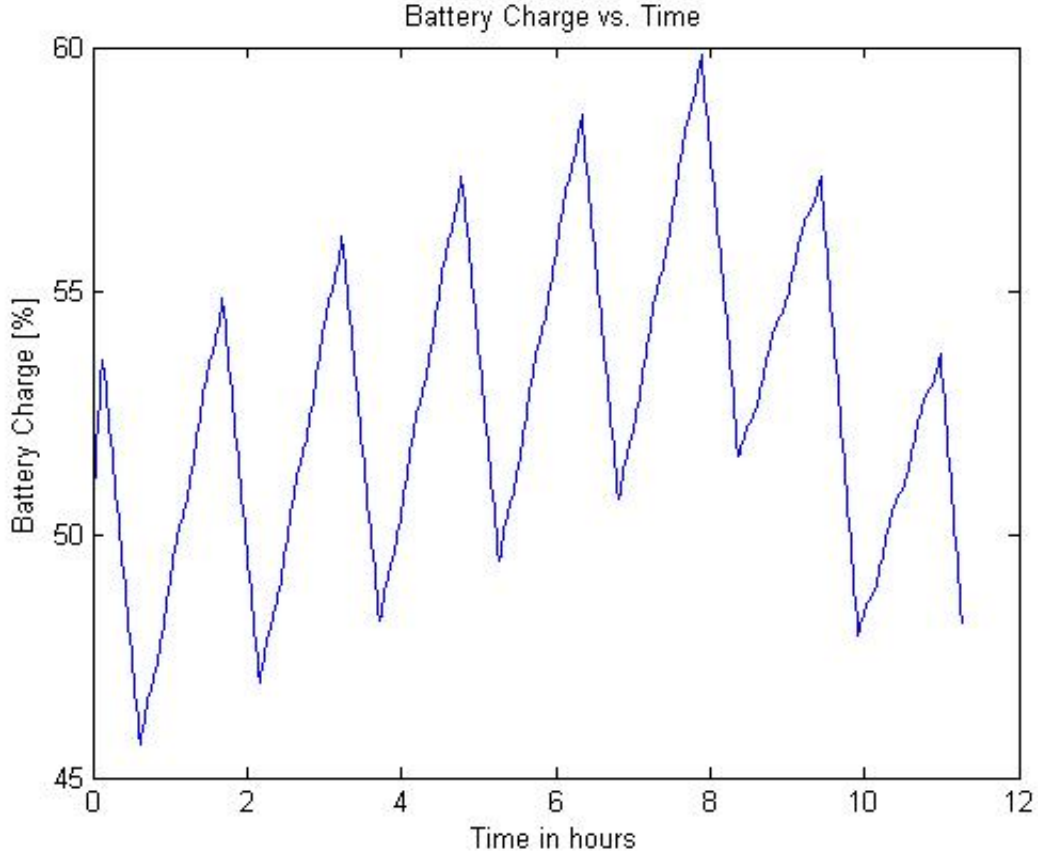


Figure 32: *Battery Charge vs. Time with $\Omega = 90^\circ$ (50% charge at time of pass)*

Assuming the limit for the satellite to switch to low power mode is 50% battery charge, this scenario observes what would happen if the satellite passes over the ground station with 50% battery charge in the worst power scenario possible. As seen in Section 5.1, for a worst case scenario, the orbit line of nodes would be essentially perpendicular to the Earth-Sun vector. This is the case for the previous orbit with $\Omega = 90^\circ$ generating an average of only 5.1 W in configuration 2.

Although the power generation is the lowest in this case, the satellite remains power positive while the spacecraft spins to achieve the target spin rate. A worst case scenario would consequently involve minimizing this power positive phase. This means having a second pass as soon as possible after the stable spin rate is achieved in order to turn on the radiometer and enter a power negative state. These conditions are all met by the orbit

studied with $\Omega = 90^\circ$ since the second pass occurs only 0.6 hours after the satellite achieves its stable spin rate. This orbit was thus simulated with an initial battery charge of 50%. Figure 32 shows that the battery in this case only manages to charge to around 55% before the radiometer is turned on and the battery starts discharging. The battery subsequently falls to 50% charge before the data acquisition is even started and no data is collected.

This worst case scenario naturally could be easily circumvented by waiting for a later pass and turning on the radiometer once the spacecraft battery is fully charged. Alternately, the satellite could wait in low power mode until it has reached a higher charge before starting to spin. This solution could take less time as the satellite is much more power-positive in the initial low-power phase. It can be deduced from Figure 32 that in the 7.5 hours required for the satellite to achieve constant spin, the battery has the time to charge 10%. Consequently, in order to achieve a full battery before turning on the radiometer, the battery has to be at least 90% charged when the satellite is instructed to switch to experiment mode, regardless of the orbit it is in. This would guarantee a minimum of 9.5 hours of continuous data acquisition.

On the other hand, in Figure 33, the satellite is in the orbit with $\Omega = 0^\circ$ with 65% initial charge when it is instructed by the ground to switch to experiment mode. In this case, it manages to charge fully during the spinning phase and while waiting for a second pass (9 hour wait). Consequently, in this particular orbit, the satellite does not need to be charged at 90% when the pass occurs to achieve the maximum possible data acquisition. Waiting for the battery to be more charged would therefore be unnecessary and would waste valuable on-orbit time in this case. It is thus important to simulate the orbit and ground passes beforehand to determine the most efficient sequence of operations.

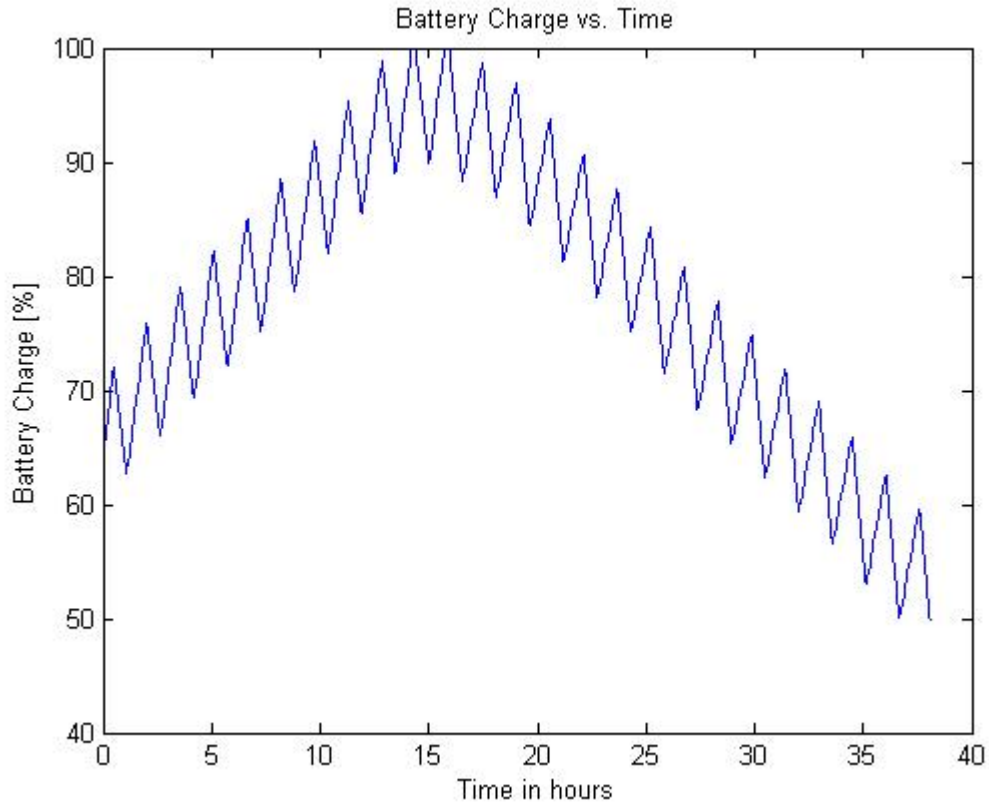


Figure 33: *Battery Charge vs. Time with $\Omega = 0^\circ$ (60% charge at time of pass)*

The amount of data that the satellite is able to collect in science mode is strongly dependent on the configuration the satellite is in and the initial state of the battery. In order to ensure a maximum amount of data is collected continuously, the battery has to be fully charged when the radiometer is turned on. This can be ensured by instructing the satellite to switch to data collection mode only when the battery is at at least 90%. Since the satellite is power positive while achieving constant spin rate, the battery charges at least 10% in that phase, dependent on the orbit. In order to reach that charge amount the satellite can be placed in low power mode before the beginning of the experiment. However, depending on the orbit, this 90% charge condition can be excessively restrictive and time consuming. Knowing the average power generation in a particular orbit and predicting satellite passes as performed with this program can then help determine a less constraining condition to begin the experiment to take full advantage of the valuable time the satellite has in orbit.

5.2.2 Radiometer Experiment Data Transfers

In addition to collecting data, an important phase of the RACE mission is the downlinking of the experiment data. In this section, the RACE spacecraft was modeled while transmitting data. The mission operations modeled in this section are represented in Figure 34. The spacecraft is placed in configuration 3 which is the optimal configuration for ground transmission. In this scenario, the radiometer is left on standby mode while the data is downlinked. This lets the spacecraft transfer quickly to science mode without waiting for a warmup period of the radiometer.

Whenever a ground pass occurs, the data is downlinked to the ground. A ground pass is assumed to occur once the satellite is visible from the UT-Austin ground station with a minimum elevation of 7.5° . The spacecraft remains ready to transfer data while the satellite maintains a greater than 50% charge (assumed to be the low power mode limit) and while the battery is not completely charged. It is assumed that once the battery is charged, the satellite would then transfer again to data collection mode. If the battery charge falls below 50%, the spacecraft would automatically switch to “Low Power Mode” which means the amount of power used by the spacecraft is at a minimum and the radiometer is off. The satellite is assumed to be spinning during the data collection and transfer phases since this does not affect the spacecraft’s ability to downlink data in configuration 3. This allows the spacecraft to maintain its spin necessary for data collection to ensure a fast transition to data collection.

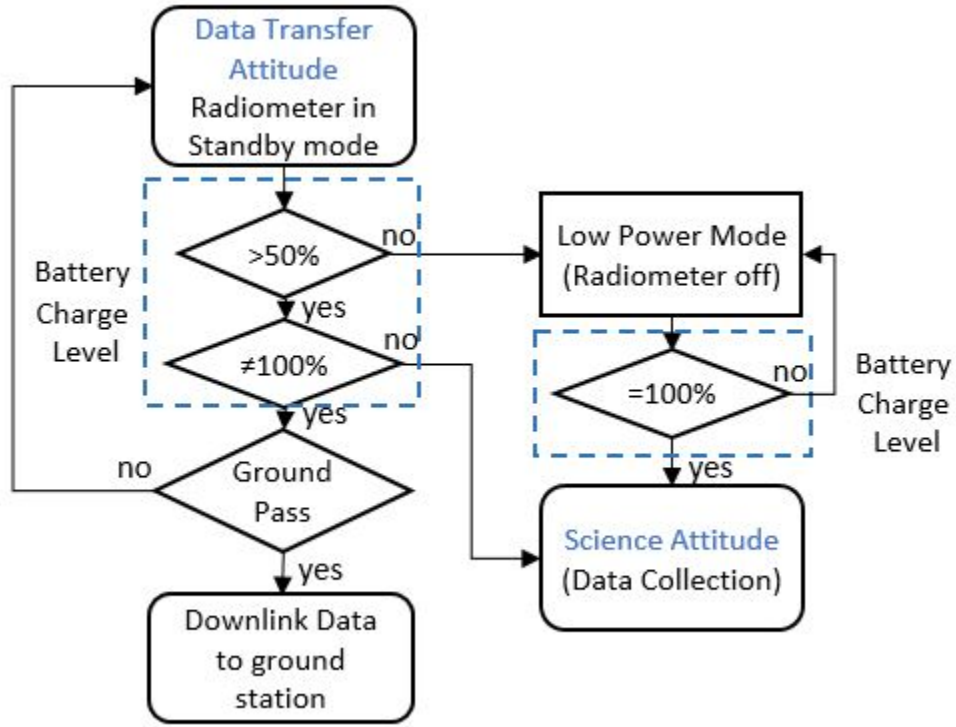


Figure 34: *Example of Data Transfer Phase Operations*

This scenario was first modeled for a line of nodes along the Earth-Sun vector $\Omega = 0$. Figure 35 shows the evolution of the power data, battery charge and satellite elevation from the UT-Austin ground station over time. From Table 8, the average power in configuration 1 with $\Omega = 0^\circ$ is around 4.2 Watts. Note that the power usage with the radiometer in standby is 5.83 W and the power used while downlinking to the ground is 9.08 W. This means that in this orbit, the satellite is continuously power negative.

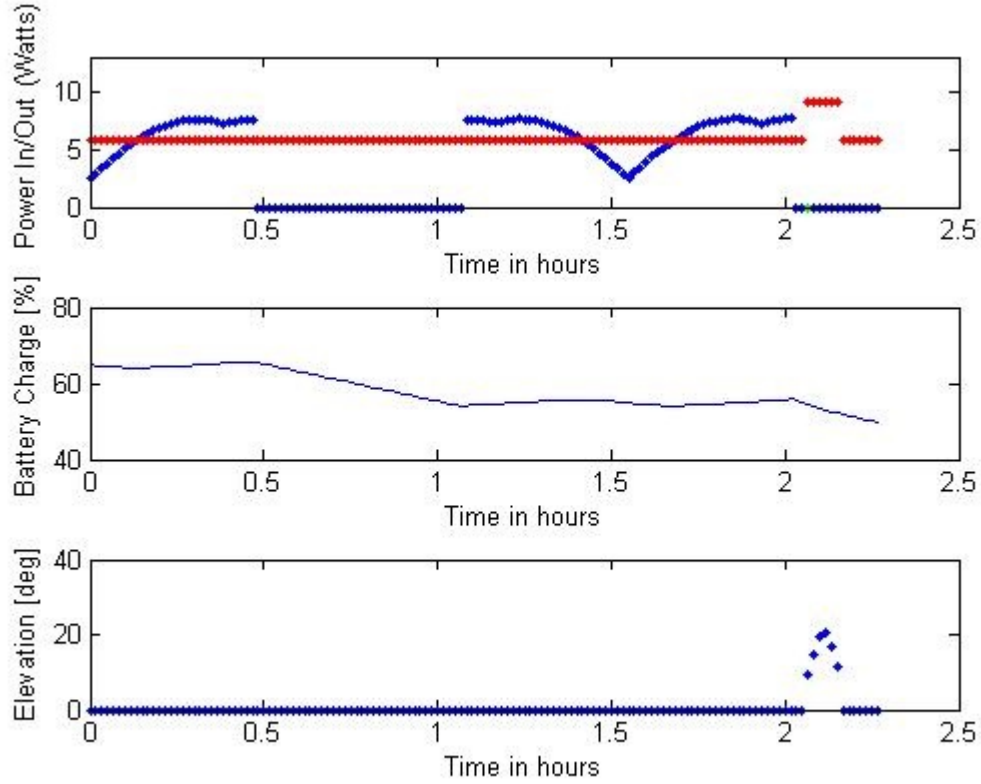


Figure 35: *RACE data transmission with $\Omega = 0^\circ$ (65% initial charge)*

Figure 35 at the top shows the power generated (blue) and expended by the spacecraft (red). In the middle, it shows the battery charge over time and at the bottom, the satellite ground passes. It is visible that the battery starts off with a 65% charge. This battery charge amount was chosen since data transmission occurs after data collection which usually significantly discharges the battery as seen in the previous section. In this simulation, an eclipse occurs after approximately 30 minutes which reduces the battery charge level to approximately 55%. Finally a pass occurs after two hours which coincides with an eclipse period. When a pass occurs, this means that the satellite is visible from the ground station (UT-Austin) and has an elevation greater than 7.5° . The satellite thus transmits data to the ground whenever it is visible from the station. This pass lasts around 6 minutes and the battery charge level falls to 50% only 2 hours and 15 minutes after the start of the data transmission phase. The spacecraft only manages to transfer 6 minutes of data before

discharging its battery to the low power limit value. This unsuccessful data transmission attempt is due to the poor power configuration yielding an average of only 4.2 Watts.

Figure 36 shows the same scenario applied to an orbit whose line of nodes is perpendicular to the Earth-Sun vector ($\Omega = 90^\circ$). In this case, in configuration 3, the average power is 6.62 W. This means the spacecraft is power positive whenever it is not in view of the ground station and downlinking data. As visible from the graphs, the spacecraft undergoes 4 different ground passes. The passes last 6, 7, 7 and 6 minutes in order of occurrence. This amounts to approximately 26 minutes of data transmission before the battery is fully charged after approximately 16 hours. It is evident that this is an ideal scenario where the spacecraft simultaneously downlinks data and charges its battery between each data acquisition phase.

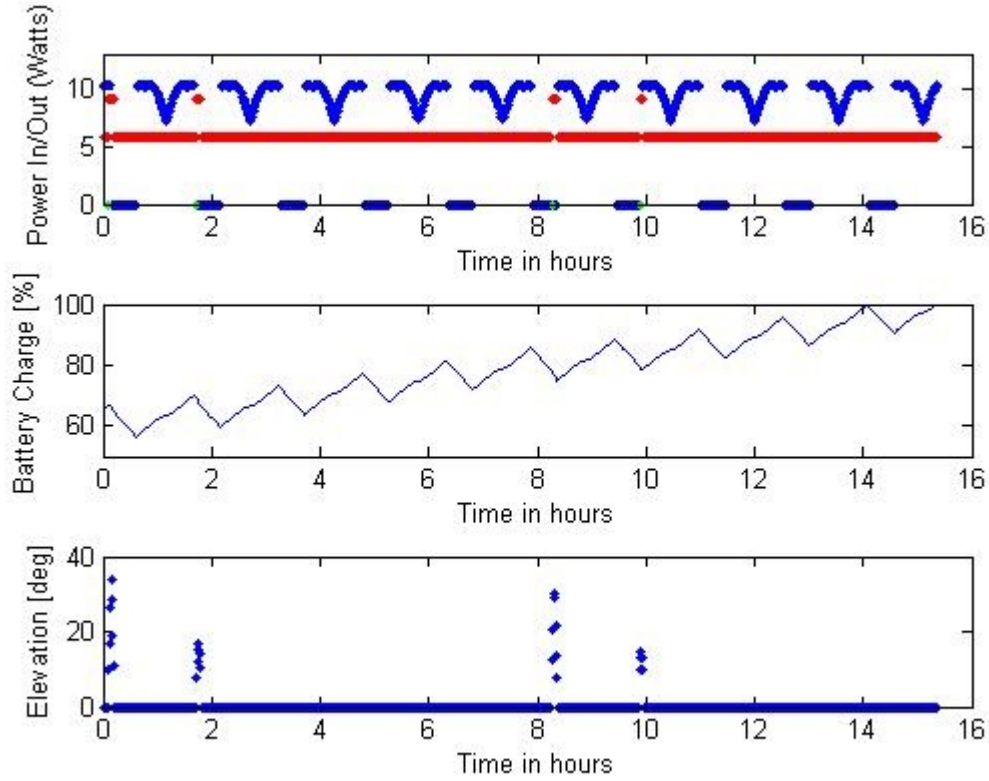


Figure 36: *RACE data transmission with $\Omega = 90^\circ$ (65% initial charge)*

Another orbit of interest would be an orbit with $\Omega = 45^\circ$ which gives an average

power generation of 5.74 W in configuration 3. This means the spacecraft is slightly power negative when it is not downlinking. The results of this test are shown in Figure 37. This scenario also discharges the battery and yields 30 minutes of data transfer before reaching 50% battery charge.

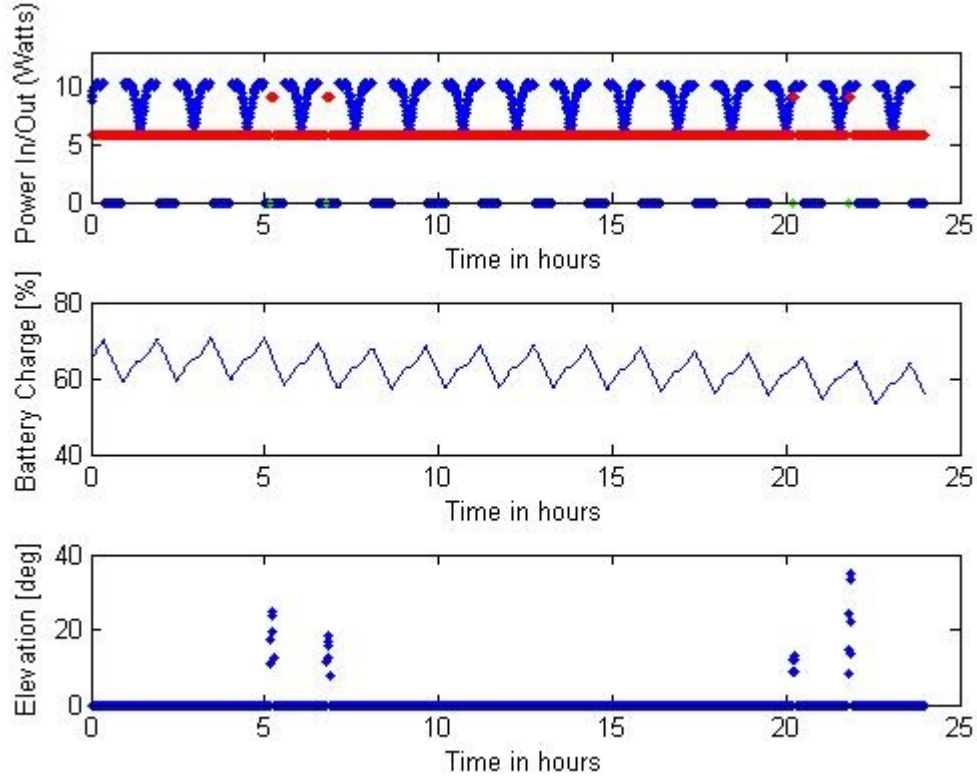


Figure 37: *RACE data transmission with $\Omega = 45^\circ$ (65% initial charge)*

Looking back at Table 8 half of the orbits studied in configuration 3 will be power negative whenever the radiometer's on stand-by. This means that after the battery is discharged, the spacecraft will have to be recharged before collecting data again. Since all orbits are power negative with the radiometer in standby in configuration 2 (data collection configuration), this means the radiometer would have to be turned off to recharge. This defeats the purpose of keeping the radiometer on while downlinking data since the radiometer will have to be turned off and warmed up again for three hours. The same scenario was thus studied with the radiometer off.

With the radiometer off, the power consumption is slightly reduced and is around 4.87 W. This means that only the orbits with line of nodes close to aligned with the Sun vector will still be power negative. The data transmission mode can thus be power positive for more orbits and the battery can be recharged faster.

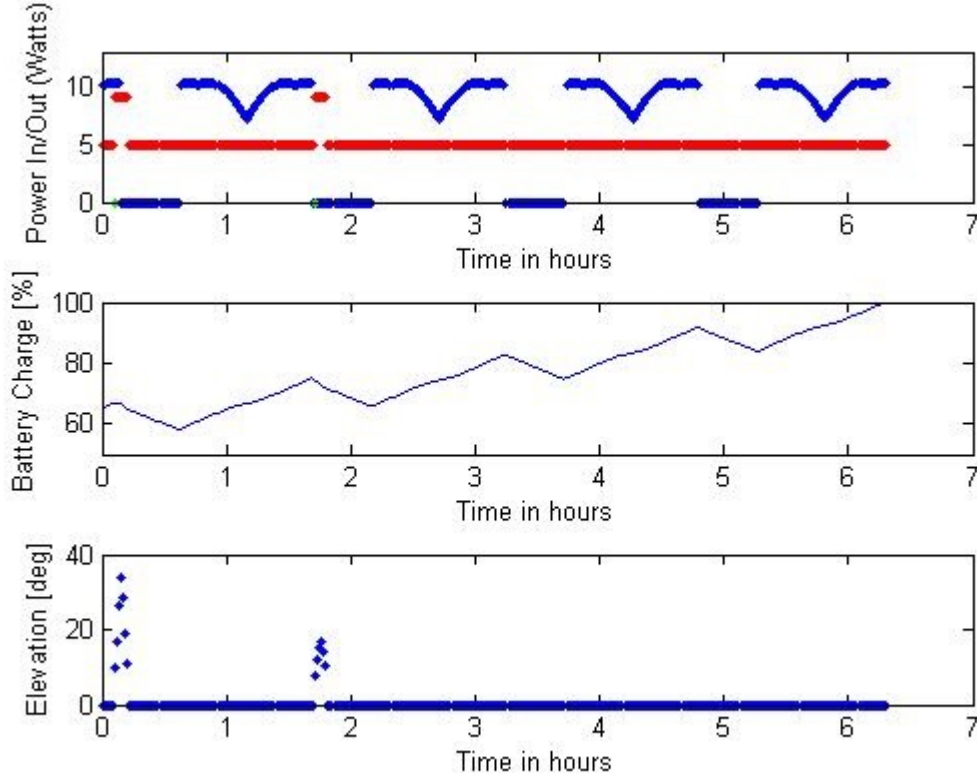


Figure 38: *RACE data transmission with $\Omega = 90^\circ$ (65% initial charge) and radiometer off*

In Figure 38, the radiometer is off throughout this phase of the mission operations and the orbit configuration is the same as in Figure 36 with $\Omega = 90^\circ$. Comparing Figures 38 and 36, the battery is recharged after little over 6 hours with the radiometer off while it took approximately 16 hours with the radiometer on in Figure 36. Since we know from Figure 36 that additional passes occur around 10 hours, the satellite can be left in data transmission configuration to achieve the additional two passes. The satellite can then switch to configuration 2 and warm up the radiometer for 3 hours, achieving the same amount of data transmission and charging the battery fully in approximately 6 hours less

than in Figure 36. Even with the 3 hour warm up time included, less time is thus spent with this mission scenario, ie. turning off the radiometer during transmission. It would thus improve the mission operations to modify the data transmission phase and turn off the radiometer fully while in that mode.

Consequently, the radiometer should be turned off during data transmission in order to maintain a power positive state for more orbits. This allows the satellite to transmit data soon after the data collection and simultaneously recharge the battery in most orbits. The subsequent time spent warming up the radiometer is compensated by the time saved in charging the battery. If the battery is not fully charged at the end of the data transmission, the satellite can then be put in low power mode to completely charge the battery before turning on the radiometer.

5.2.3 RACE Recommendations

In summary, Figure 39 shows the recommended RACE mission operations for the radiometer experiment phase of the mission. We have previously shown that since the spacecraft is power negative with the radiometer on, the battery should be fully charged before the instrument is turned on. Furthermore, we showed that it is more advantageous to turn off the radiometer when downlinking data rather than leaving it on standby. Depending on the orbit the spacecraft is in, the ground station may choose to either downlink data between each data acquisition phase if the data transfer attitude generates more power or leave it in the science configuration to recharge. In this scenario the low power limit is set to 50% battery charge level which may be adjusted. In science attitude, the spacecraft prioritizes data collection, switching on the radiometer as soon as the batteries are charged. The spacecraft may switch to data transmission if it receives a ground command. On the other hand, in data transfer attitude, the spacecraft stays in that configuration as long as a ground command doesn't transfer it back to science mode.

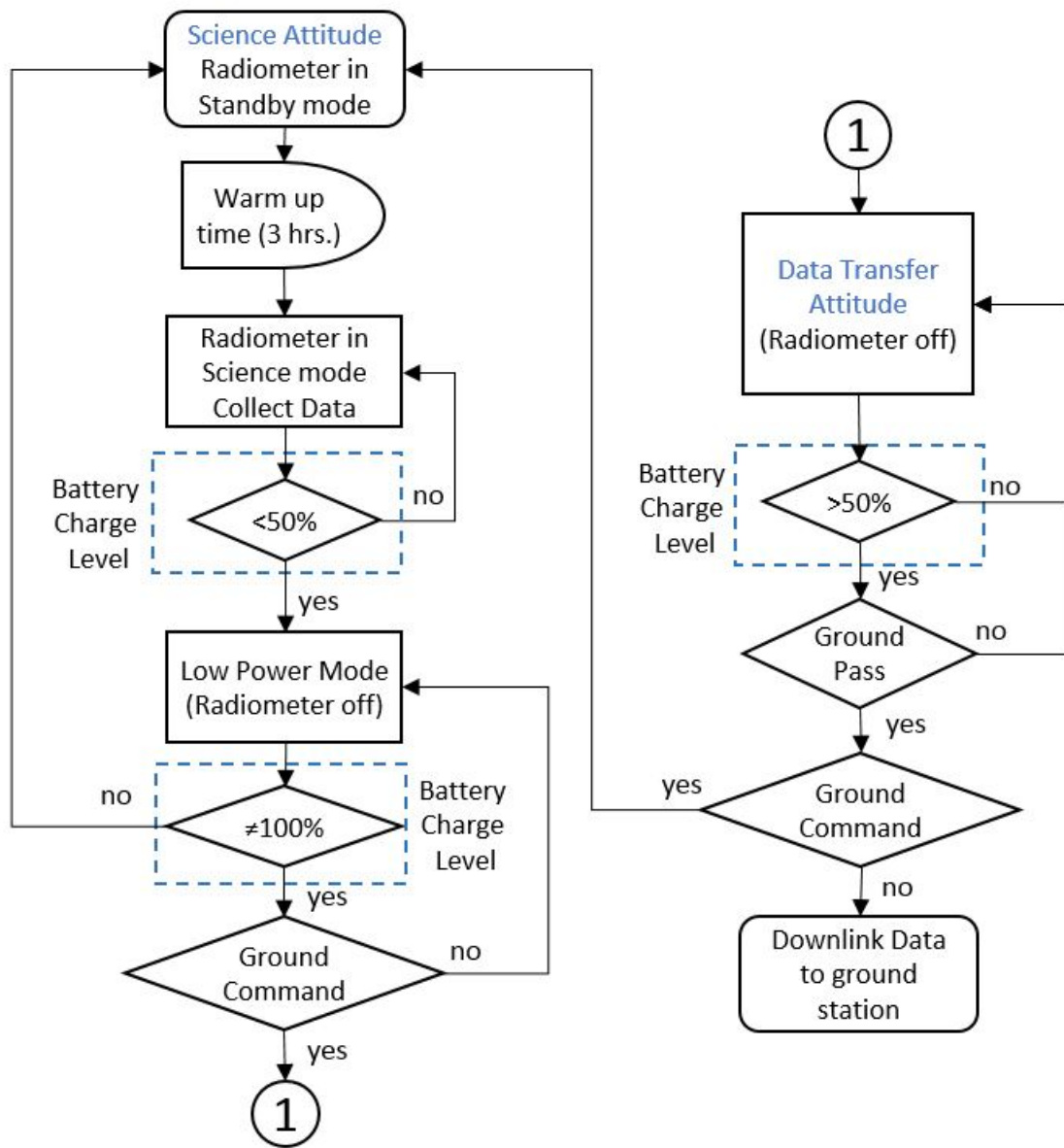


Figure 39: Recommended Mission Operations

6 Conclusion

In conclusion, a versatile mission design tool was created with the capability to provide an overview of mission operations to improve mission planning. It was shown that the tool can simulate a spacecraft orbit and its power generation over time as well as predict ground station passes. Provided with power usage data for a specific system, it can be used to simulate a particular mission scenario with power budget calculations.

The tool capabilities were demonstrated through the simulation of the RACE spacecraft operations. This then led to the conclusion that the power generation for the RACE spacecraft is dependent on the orbit plane orientation with respect the sun. A set of power tables were thus generated to reference once a particular launch orbit is fixed. These may then be used to determine how much data can be collected continuously and how to meet the data collection requirements. Further analysis showed that the RACE radiometer payload should be turned off between each data acquisition phase in order to recharge the spacecraft battery. Analysis of the tool results thus led to new recommendations for the mission and an improved and comprehensive diagram of the mission operations was created.

Finally, the tool is designed so that a future user may easily modify and create new mission scenarios and add capabilities. Future improvements should include better battery charge and discharge models as well as cell power generation models.

References

- [1] "About SPICE." About Spice. The Navigation and Ancillary Information Facility, n.d. Web. 25 Nov. 2013. <<http://naif.jpl.nasa.gov/naif/aboutspice.html>>.
- [2] Curtis, Howard D. *Orbital Mechanics for Engineering Students*. N.p.: Butterworth-Heinemann, 2005. Print.
- [3] Bate, Roger R., Donald D. Mueller, and Jerry E. White. *Fundamentals of Astrodynamics*. New York: Dover Publications, 1971. Print.
- [4] "Heavens-Above." Heavens-Above. DLR German Aerospace Center, n.d. Web. 04 Oct. 2013. <<http://www.heavens-above.com/>>.
- [5] Tapley, Schutz, and Born, "Statistical Orbit Determination," Elsevier Academic Press, 2004
- [6] CNES Celestlab Space Mechanics Toolbox. Computer software. Scilab 5.4.1, n.d. Web. <<http://forge.scilab.org/index.php/p/celestlab/>>.
- [7] Kenyon, I. R. "Radiation Terminology." *The Light Fantastic: A Modern Introduction to Classical and Quantum Optics*. Oxford: Oxford UP, 2011. N. pag. Print.
- [8] U.S. Standard Atmosphere, 1976, U.S. Government Printing Office, Washington, D.C., 1976
- [9] Eagle, David. "Orbital Mechanics with MATLAB." *Orbital Mechanics with MATLAB*. N.p., n.d. Web. 26 Oct. 2013. <<http://www.cdeagle.com/ommatlab/toolbox.pdf>>.
- [10] "Ultra Triple Junction (UTJ) Solar Cells." SPECTROLAB. N.p., n.d. Web. <<http://www.spectrolab.com/DataSheets/cells/PV%20UTJ%20Cell%205-20-10.pdf>>.

- [11] Lightsey, E. G. "RACE." Lightsey Research Group. N.p., n.d. Web. 30 Nov. 2013. <<http://lightsey.ae.utexas.edu/research/race/>>.
- [12] "Radiometer Atmospheric CubeSat Experiment (RACE)." NASA Jet Propulsion Laboratory. N.p., n.d. Web. 30 Nov. 2013. <<http://phaeton.jpl.nasa.gov/external/projects/race.cfm>>.
- [13] Racette, Paul E., and Coauthors, 2005: Measurement of low amounts of precipitable water vapor using ground-based millimeterwave radiometry. *J. Atmos. Oceanic Technol.*, 22, 317337.
- [14] "Nanopower Modules." Cubesat and Nano-satellite Solutions. GOMSPACE, n.d. Web. 30 Nov. 2013. <<http://gomspace.com/index.php?p=products-p31u>>.